HHS Public Access

Author manuscript

Expert Opin Drug Deliv. Author manuscript; available in PMC 2020 January 01.

Published in final edited form as:

Expert Opin Drug Deliv. 2019 January ; 16(1): 7–26. doi:10.1080/17425247.2019.1551875.

Use of computational fluid dynamics deposition modeling in respiratory drug delivery

P. Worth Longest[1,2,*], **Karl Bass**[1], **Rabijit Dutta**[1], **Vijaya Rani**[1], **Morgan L. Thomas**[1], **Ahmad El-Achwah**[1], and **Michael Hindle**[2]

[1]Department of Mechanical and Nuclear Engineering, Virginia Commonwealth University, Richmond, VA, USA

[2]Department of Pharmaceutics, Virginia Commonwealth University, Richmond, VA, USA

Abstract

Introduction: Respiratory drug delivery is a surprisingly complex process with a number of physical and biological challenges. Computational fluid dynamics (CFD) is a scientific simulation technique that is capable of providing spatially and temporally resolved predictions of many aspects related to respiratory drug delivery from initial aerosol formation through respiratory cellular drug absorption.

Areas Covered: This review article focuses on CFD-based deposition modeling applied to pharmaceutical aerosols. Areas covered include the development of new complete-airway CFD deposition models and the application of these models to develop a next generation of respiratory drug delivery strategies.

Expert Opinion: Complete-airway deposition modeling is a valuable research tool that can improve our understanding of pharmaceutical aerosol delivery and is already supporting medical hypotheses, such as the expected under-treatment of the small airways in asthma. These complete-airway models are also being used to advance next generation aerosol delivery strategies, like controlled condensational growth. We envision future applications of CFD deposition modeling to reduce the need for human subject testing in developing new devices and formulations, to help establish bioequivalence for the accelerated approval of generic inhalers, and to provide valuable new insights related to drug dissolution and clearance leading to microdosimetry maps of drug absorption.

[*]**Correspondence:** P. Worth Longest, Virginia Commonwealth University, 401 West Main Street, P.O. Box 843015, Richmond, VA 23284-3015, USA, Phone: (804)-827-7023, Fax: (804)-827-7030, pwlongest@vcu.edu.

Declaration of interest

Virginia Commonwealth University is currently pursuing patent protection of excipient enhanced growth aerosol delivery, aerosol generation devices and patient interfaces, which if licensed, may provide a future financial interest to the authors. The authors have no other relevant affiliations or financial involvement with any organization or entity with a financial interest in or financial conflict with the subject matter or materials discussed in the manuscript apart from those disclosed.

Reviewer disclosures

Peer reviewers on this manuscript have no relevant financial or other relationships to disclose.

Keywords

Pharmaceutical aerosols; inhalers; CFD simulations; airway models; aerosol deposition; aerosol dosimetry; bioequivalence; complete-airway modeling; whole-lung CFD modeling

1. Introduction

The delivery of pharmaceutical aerosols to the lungs for the treatment of lung diseases and through the lungs for the treatment of systemic conditions remains challenging for many medications. The breakup of liquid or powder into droplets or particles that are small enough to be efficiently inhaled and reach the lungs requires a surprising amount of energy [1]. This breakup or dispersion energy typically results in high airflow momentum and turbulence, which has the unintended consequence of large drug loss fractions in the inhaler and extrathoracic airways [2] reducing the amount of drug available for deposition in the lungs. The lung airways beginning with the trachea form a complex bifurcating network that efficiently filters incoming particulate matter and protects the sensitive alveolar region. Within this bifurcating network, effective drug action requires that the required dose of the inhaled medication be delivered to the target region. However, this site of action and the required dose varies depending on the disease or delivery application considered. For example, beta-adrenergic bronchodilators used for the treatment of asthma are most effective in the tracheobronchial airways [3]. The tracheobronchial airways at first appear to be a simple target for asthma medications, such as bronchodilators and corticosteroids; however, the smallest tracheobronchial airways are currently undertreated with inhaled corticosteroid medications in a majority of asthma patients [4, 5]. Other examples include administration of inhaled antibiotics, which should provide a uniform concentration of drug within the airway surface liquid or at least maintain values above the minimum inhibitory concentration [6, 7]. Inhaled surfactants are intended to be delivered primarily past the tracheobronchial region into the alveoli [8]. Once pharmaceutical aerosols are deposited, clearance mechanisms immediately starts to deactivate and remove the drug [9]. At the same time, drug molecule dissolution and absorption into the lung tissue are occurring [10]. For most commercially available inhalers, only approximately 15 to 40% of the aerosolized drug reaches the adult lung [11, 12]. Of this fraction, only a small percentage, which may be less than 1%, is typically deposited in an airway region, like the small tracheobronchial airways [13]. Absorption of the deposited drug then varies widely depending on the physicochemical properties of the drug molecule and formulation, and may be as low as 1% of the deposited dose for some hydrophobic medications [14, 15].

To better understand the complex process of respiratory drug delivery, aerosol deposition models have been in development for decades. As reviewed by Longest and Holbrook [16], the classic approach of algebraic whole-lung modeling can be sub-divided into semi-empirical and one-dimensional (1D) models. Semi-empirical models provide correlations for predicting whole-lung deposition or regional deposition based on fitting empirical data as a function of analytical parameters [17]. Finlay and Martin [18] reviewed semi-empirical models and new developments in predicting aerosol deposition in the respiratory tract with comparisons to *in vivo* data. Overall, semi-empirical models can accurately match the

amount of inhaled drug that reaches the lungs. However, information is not provided regarding how this medication is distributed within the airways.

Whole-lung 1D models assume either a single path [19] or stochastic [20] lung geometry and employ algebraic expressions for aerosol deposition by different physical mechanisms such as sedimentation, impaction, and diffusion [21]. As a recent example of a whole-lung 1D model, the study of Katz et al. [22] compared model predictions to a newly developed high resolution *in vivo* lung deposition dataset [23] and found limitations in the model's predictive ability to capture mouth-throat (MT) deposition and to resolve deposition within the tracheobronchial region. Whole-lung 1D predictions in the alveolar region and exhaled mass fraction are also frequently inaccurate [24, 25, 26].

A challenge with both semi-empirical and 1D models is correcting the predictions for a number of factors related to the transport and deposition of pharmaceutical aerosols. Corrections are typically needed for factors such as jet and spray momentum associated with inhaler use [2], hygroscopic condensational and evaporative effects resulting in size change of droplets [27], turbulence [28], bifurcating geometries [29], and realistic alveolar structures [30]. Corrections can account for some of these factors [31]; however, this is often difficult and may rely on correlations developed from CFD simulations [32] or *in vitro* experiments [33]. Further details of these more traditional modeling approaches are provided in Longest and Holbrook [16].

An alternative approach to algebraic deposition modeling is the use of computational fluid dynamics (CFD) applied to gas flow and aerosol deposition in the respiratory airways. CFD was originally developed by engineers for the aerospace industry, and continues to advance and evolve for a variety of applications [34, 35]. At its core, this scientific simulation approach divides a realistic three-dimensional (3D) flow geometry into small control volumes, or voxels. The partial differential equations governing mass, momentum and energy transport are formed for each control volume, and solved in a coupled manner. A typical CFD mesh contains millions of control volumes, requiring the governing equations to be formed into large matrices (theoretically containing trillions of elements) and solved using efficient matrix solution algorithms. In this manner, CFD solutions can fully resolve all aspects of a flow field including a particle or droplet phase in 3D space and over time. As a scientific tool, CFD was initially applied to determine particle deposition in the respiratory airways on a consistent basis over 20 years ago with the pioneering work of Balashazy and Hofmann et al. [36], Finlay et al. [37], Kimbell et al. [38], Kleinstreuer et al. [39], and Martonen et al. [40].

CFD models of respiratory drug delivery have a number of advantages compared with semi-empirical and 1D whole-lung approaches. CFD simulations are based on solution of the underlying transport equations, which can directly account for factors such as transient flow, turbulence and turbulent particle dispersion, hygroscopic particle size change, and fluid-wall interactions in complex geometries. With CFD simulations, realistic airway geometries are employed, which are necessary to account for deposition in complex structures like the larynx [41], airway bifurcations, and constricted airways [42]. Highly realistic models of the alveolar region including wall motion are also possible [43]. Considering pharmaceutical

aerosols, CFD simulations can directly predict the effects of jet and spray momentum on an aerosol as it is emitted from an inhaler into the mouth-throat and upper tracheobronchial airways [2]. Limitations of CFD models include complexity in capturing the physics associated with pharmaceutical aerosol generation and delivery, difficulty in resolving flow dynamics in the vast expanse of the bifurcating airways, and computational expense. As a result, CFD models are typically limited to sections of the respiratory tract [44, 45, 46, 47, 48], such as from the oral cavity to as far as approximately the sixth airway generation [44]. CFD models of different regions including the extrathoracic, tracheobronchial and alveolar airways are more completely reviewed by Longest and Holbrook [16].

Primary areas in which CFD has been applied to respiratory drug delivery include (*i*) simulating aerosol formation, (*ii*) aiding inhaler design and optimizing device performance, and (*iii*) airway deposition modeling, as illustrated in Figure 1. Aerosol formation may include the breakup of liquids into droplets or powders into discrete particles. Due to physical complexity and coupling of the breakup process, these simulations are currently limited to small regions on the millimeter scale, or to even just a few particles or a single particle aggregate [49, 50]. Excellent overviews of simulating aerosol formation and multiscale modeling are available from Sommerfeld et al. [51] and Wong et al. [52]. Considering inhaler and device design, CFD has been implemented to understand aerosolization performance, reduce device depositional drug loss, and improve delivery of the aerosol through the extrathoracic region. This topic was recently reviewed by Ruzycki et al. [53] and Wong et al. [52].

The focus of this review is CFD applied to airway deposition modeling, which is the third key area illustrated in Figure 1. Previous reviews have covered this topic with a focus on regional deposition modeling [16]. However, this field has rapidly evolved over the past 5 to 10 years, leading to major advances including complete-airway simulations and successful comparisons with *in vivo* gamma scintigraphy data in human subjects. Due to the breadth of this area, models simulating nasal sprays and nasally targeted aerosols are not included, except for when they are needed to illustrate a new modeling approach. This review first covers new findings from regional airway simulations that have physiological significance for the delivery of pharmaceutical aerosols. Progress in the development of complete-airway deposition models is then described, including validation with concurrent *in vitro* and previous *in vivo* experimental studies. Applications of these new complete-airway simulations can be divided into (*i*) the evaluation of existing inhalers and (*ii*) development of new respiratory drug delivery strategies, with recent findings reviewed in each area. The use of CFD deposition models to improve respiratory drug delivery in challenging scenarios is presented for the selected cases of infants, children and diseased lungs. Finally, we present our opinion related to current model contributions, necessary model improvements and new modeling directions.

2. State of the art in regional airway aerosol deposition modeling

Regional airway models have been used to evaluate sections of the respiratory tract including the mouth-throat and upper tracheobronchial regions [13, 27, 28, 54, 55], alveolar geometries [43, 56], and complete-airway models through approximately generation B8 with

some branches extended to B16 [57, 58, 59, 60]. As reviewed by Longest and Holbrook [16], early contributions of these regional models were the quantification of focal points of aerosol deposition within bifurcations, or hot spots, associated with deposition by impaction and diffusion. Whether a drug is rapidly or slowly absorbed, the initial deposition sites are expected to influence the absorption profile over time and spatially within each lung geometry. For quickly absorbed medications, that can dissolve in airway surface liquid and then be absorbed by the respiratory epithelium, the initial deposition site is expected to strongly influence the spatial absorption profile, leading to uneven microdosimetry patterns [41, 42, 61, 62].

Regional models of the mouth-throat geometry for pharmaceutical aerosols have frequently highlighted unwanted oropharyngeal deposition due to turbulent jets and aerosol spray momentum arising from inhalers [2, 63, 64]. As described by Finlay and Martin [65], these models can be used to develop quantitative algebraic correlations that can predict mouth-throat deposition based on known input parameters such as inhaler flow rate and aerosol inlet jet diameter. Regional mouth-throat models have also been used to quantify reduced extrathoracic depositional loss expected with next generation delivery devices that reduce turbulence and spray momentum [27].

Beyond the oral airway, simulations of the laryngeal jet illustrate an additional hurdle to the lung delivery of pharmaceutical aerosols [41, 46, 66]. Xi et al. [41] reported that due to flow instabilities, the laryngeal jet was not centrally located within the trachea, but preferentially attached to the tracheal side wall, which can be referred to as the Coanda effect from fluid mechanics [41]. This asymmetrical pattern increases recirculation and turbulence in the trachea, which results in increased aerosol depositional loss. Furthermore, the laryngeal jet pattern was found to strongly influence the distribution of aerosol particles within the lung lobes and shift maximum drug surface concentration away from the main carina and to the lobar-to-segmental bifurcations [41]. These findings highlight the importance of including the laryngeal structure in CFD and *in vitro* analysis of aerosol delivery to the lungs. Using a similar regional airway geometry, Lambert et al. [44] studied regional aerosol distribution in a patient-specific CFD model, which began with the oral airway and included six generations of the tracheobronchial region. Their results showed that the left lung received a higher fraction of aerosol mass despite the right lung receiving the higher airflow ventilation, which they attributed to the effects of the laryngeal jet. Recently, Miyawaki et al. [67, 68] also reported the importance of correctly modeling the laryngeal jet for accurate prediction of gas flow and aerosol delivery in human lungs.

Recent advances in 3D imaging and numerical simulations have facilitated the development of physically realistic models of pulmonary alveolar airways at sub-millimeter scales. Sznitman and co-workers have developed an acinar geometry from repeating polyhedral-shaped alveolar cavities that mimic the underlying space-filling acinar morphology [43, 69, 70]. Their alveolar CFD model has been employed in understanding aerosol deposition characteristics in diseased emphysematous acini [71] and targeted alveolar deposition using magnetic particles [72]. Recently, they developed a new model [73] for particle deposition in the anatomically realistic heterogeneous acinar environment by employing the algorithm of Koshiyama and Wada [74], which captures the complete alveolar geometry of human acinar

morphometry. Talaat and Xi [75, 76] developed a CFD model for transient particle deposition in terminal alveoli using rhythmically moving alveolar boundary conditions in phase with measured chest wall motions and tidal volumes and showed that the periodic alveolar wall motion leads to enhanced particle dispersion that reduces particle deposition in the alveoli. Sera et al. [77] developed a pulmonary acinar model based on high-resolution CT scans of a mammalian lung and showed that the particle deposition in the realistic pulmonary acinar model is higher than in an idealized model. In highly complex but smaller scale models, of for example one alveolus, the importance of hysteresis in alveolar expansion and contraction has been demonstrated [78].

In contrast to passive tidal breathing, the delivery of pharmaceutical aerosols typically employs the use of deep inhalation volume [79], with either fast or slow rate of inhalation, followed by a breath-hold period. As described in later sections detailing the development of complete-airway models, Khajeh-Hosseini-Dalasm and Longest [56] used a realistic space-filling representative model of a complete acinar region and developed correlations for alveolar particle deposition consistent with deep volume inhalation and a breath-hold periods.

3. Validation of regional airway model predictions with *in vitro* experimental data

Comparisons of CFD predictions with *in vitro* experimental data for pharmaceutical aerosol deposition were thoroughly covered by Longest and Holbrook [16], with additional comparisons having been reported since this previous review. The *in vitro* experiments employ a realistic airway geometry of the mouth-throat which can be extended up to generation B3 of the tracheobronchial region. Inhalation from the pharmaceutical inhaler is simulated using a realistic inhalation profile selected as appropriate for the test inhaler. Drug deposition in the inhaler, on the airway model and the amount of drug penetrating the extrathoracic region is quantified to estimate regional deposition and the lung delivery of the aerosol. Briefly, considering regional airway geometries with multiple inhaler types, successful comparisons have been made between CFD predictions and concurrent *in vitro* measurements of deposited drug mass for dry powder inhalers (DPI) [13, 28, 54, 55, 64, 80, 81], pressurized metered dose inhalers (pMDI) [13, 63, 80] and soft mist inhalers (SMI) [2, 27, 82, 83, 84, 85, 86]. Successful quantitative comparisons of aerosol drug deposition have been reported in the inhaler alone [83, 84], with a focus on quantitative device design, as well as in the inhaler and upper airways including the mouth-throat region [27] and sometimes extending through the third respiratory bifurcation [13, 28, 55]. Highly localized deposition has also been compared between CFD predictions and *in vitro* experiments that include individual particle counting in lower airway bifurcation regions [87, 88, 89]. Recently, the study of Holbrook and Longest [90] illustrated the effects of *in vitro* surface preparation characteristics on local aerosol deposition and the associated comparisons with CFD predictions on a millimeter scale grid with individual particle counting. In comparing pharmaceutical aerosol deposition between simulations and experiments, it is often critical to correctly capture inhaler effects including turbulent jets and aerosol spray momentum [2, 64, 80, 91]. Additional factors may include droplet evaporation and hygroscopic growth,

electrostatic charge and two-way coupling. To correctly model turbulence, it is important to use an anisotropic turbulence model or to correct turbulence predictions in the near-wall region [27, 54, 81, 82, 92, 93]. In comparisons of CFD model predictions and *in vitro* results, relative errors are typically approximately 10% or less, often averaged over multiple regions (e.g., inhaler, mouth-throat, and upper tracheobronchial airways). Absolute difference errors, which may be more directly applicable to the amount of drug mass deposited, are typically 5% or less. High quality agreement is often assumed when the CFD predictions of drug mass fall within the standard deviation bars of the experimental data across multiple locations.

4. Development of complete-airway deposition models

Developing numerical models of the entire respiratory airways, from the nose, mouth, and throat through the terminal bronchioles and to the alveoli, as illustrated in Figure 2, poses multiple challenges. Division of the flow at each bifurcation, combined with decreasing airway diameters, results in a decrease in Reynolds number through the airways. This means the flow may enter the extrathoracic airways under fully-turbulent conditions, and then move through transitional and laminar regimes in more distal regions of the lung. The importance of transient forces, characterized by the Womersley number, also decreases as flow progresses from the upper to lower airways. Therefore, a transient formulation of the Navier-Stokes equations may not be necessary in all conducting airways. Furthermore, distal regions of the lung are more compliant, so the movement of wall boundaries and the associated change in domain volume must be considered. This is especially true when modeling the alveoli, as flow is drawn into the lungs through expansion of these structures. Finally, the sheer number of airway generations in the human lung (over 1 million assuming an average of 20 bifurcation levels) makes it impossible to model all possible flow paths with CFD using current computational resources.

Our group has published a series of studies on the development of CFD methods to understand flow and particle deposition patterns in complete-airway models. The stochastic individual path (SIP) method [13, 28, 55, 94, 95] aims to overcome many of the issues outlined above, and has been successfully validated against both *in vitro* [13, 28, 55, 96], and *in vivo* [97, 98] data. Figure 3 represents a sample *in vivo* validation of complete-airway model predictions of deposited drug mass compared with the *in vivo* gamma scintigraphy study of Newman et al. [99] employing an earlier version of the Respimat inhaler [98].

The SIP approach models the airways in three individual sections, from the mouth-throat to bifurcation three (MT-B3), bifurcation four to seven (B4–B7), and bifurcation eight to 15 (B8–B15). The MT-B3 region is a complete airway model developed from computed tomography (CT) scans [96]. The bifurcations in the B4–B7 and B8–B15 regions are also anatomically accurate, with physiological bifurcation data based on anatomical studies [100] and airway dimensions based on measurements from Yeh and Schum [101] or other lung morphometry datasets [1, 102, 103, 104, 105, 106]. These models are combined with our expanding alveolar model [56] to evaluate flow and aerosol deposition patterns in the entire lung (Figure 2). Separating the airways into three distinct regions overcomes the issues with changes in length scale and flow distribution, as each region can be modeled in a coupled

series. The MT-B3 region typically requires the use of a turbulence model and time-dependent simulations due to high Reynolds and Womersley numbers; whereas the B4–B7 and B8–B15 regions use laminar or turbulent and steady-state flow conditions, depending on the inhalation volume and flow rate. Multiple SIP geometries can be followed through each lobe to determine lobar deposition data [55], and previous work has shown that the lower-left lobe provides a representative average of total lung deposition [28].

A fundamental element of the SIP complete-airway approach is the application of the SIP unit geometries to model deposition in the tracheobronchial region. The tracheobronchial airways from approximately B3 through B16 (terminal bronchioles) contain approximately 130,000 airways. Considering that on the order of 100,000 control volumes at a minimum are required to adequately resolve inertial particle deposition in a single bifurcation [107, 108], we feel that full simulation of deposition in the tracheobronchial region is not practical. The alternative is using SIP geometries, which follow randomly generated paths into each lung lobe, similar to the Monte Carlo technique developed by Koblinger and Hofmann [25] for 1D complete-airway models. To generate the SIP pathways, after each bifurcation one daughter branch is continued and one is not. Realistic SIP pathway geometries are defined using a space-filling algorithm in geometric models of each lung lobe. In this manner, we capture the effect of each bifurcation on deposition in a spatially accurate mapped 3D geometry. We have found that the number of SIP pathways required depends on the desired level of deposition resolution and the state of the lung airways in terms of disease state. Dividing deposition into only three lung regions, in order to match 2D gamma scintigraphy deposition data, required only one SIP in each lung lobe [97, 98]. In contrast, for more refined predictions, the stochastic nature of SIP modeling should be employed. As illustrated in Tian et al. [55], multiple pathways are simulated into each lung lobe with ensemble averages of regional deposition taken across the SIP geometries. Sufficient SIP pathways are taken until the ensemble average converges to within a defined tolerance for the resolution of deposition predictions that is desired. In this manner, lung generation level predictions of deposition and particle localization within bifurcations (microdosimetry) can be achieved in a spatially accurate manner. A complete-airway ventilation model, as described by Tawhai et al. [109] can be coupled with the 3D CFD model of particle transport and deposition to improve simulations of heterogeneous lung ventilation. As described by Tian et al. [55], the SIP approach reduces simulation time compared with modeling all airway branches by multiple orders of magnitude. In addition to more refined predictions, the simulation of many SIP airway geometries with a coupled lung ventilation model will be required for simulating deposition within diseased airways.

Kleinstreuer and co-workers have made numerous contributions in the field of complete-airway CFD with their whole-lung airway model (WLAM) [110, 111, 112, 113, 114, 115], which has also been validated against *in vitro* [112, 113] and *in vivo* [111, 114, 115] particle deposition data. Similar to the SIP method, WLAM uses a multiscale approach and separates the airways to model discrete bifurcation regions. The extrathoracic and tracheobronchial region begins with geometry obtained from patient specific CT scans down to approximately the third bifurcation. Thereafter, anatomically accurate triple bifurcation units (TBUs) are used to model generations four through 21, with spherical alveoli introduced with increasing

density from generations 16 to 21. The whole lung model ends with a double bifurcation unit that represents generations 22 and 23, and a terminal alveolar sac.

Other studies of note in this field include a lung model of the first 17 generations from Islam et al. [116], and work from the Lin group who employ a hybrid 3D/1D method where CFD is applied in the 3D upper airway [117, 118, 119]. Finally, an interesting method developed by the University of Auckland uses a volume-filling, branching tree algorithm to define the large number of bifurcations in the lower airways, with dimensions based on anatomically accurate morphometric data [109, 120, 121].

5. Evaluation of existing inhalers

Previous studies have reviewed how airflow dynamics generated within inhalers can influence aerosol transport and deposition in the mouth-throat region and subsequent turbulence levels and aerosol deposition in the lungs [16, 65]. In this section we focus on initial CFD studies with spray inhalers that demonstrated the potential of CFD modeling followed by more recent findings arising from studies that have considered commercial products coupled with complete-airway models. Thorough reviews of turbulent jets arising from DPIs and the subsequent increase in mouth-throat particle deposition are provided in Finlay and Martin [65] and Ruzycki et al. [53].

Kleinstreuer et al. [63] were the first to simulate a MDI coupled with a representative mouth-throat geometry and predict the effects of inhaler spray momentum on aerosol transport and deposition. CFD results were in good agreement with both *in vitro* and *in vivo* studies in terms of inhaler and mouth-throat deposition as well as lung delivery of the aerosol. The CFD model successfully captured lung delivery differences for the two main types of MDIs (CFC and HFA) and reduced mouth-throat deposition with the use of a spacer. The CFD geometry did not extend beyond the mouth-throat and it was assumed that all aerosol exiting the upper airway geometry deposited in the lungs. Vinchurkar et al. [122] considered an HFA MDI coupled with patient-specific mouth-throat models extending through approximately bifurcation B5 to B9. Details of the spray simulation in the vicinity of the 0.5 mm MDI nozzle were not provided and it was assumed that aerosol deposited once it entered the lungs. Based on comparisons with concurrent *in vivo* studies, the average lung delivery efficiency of the six patient-specific models predicted by the CFD simulations matched the average experimental results. Both the studies of Kleinstreuer et al. [63] and Vinchurkar et al. [122] illustrated how CFD simulations that included the inhaler, physics of the inhaler's effects on airflow, and an upper airway geometry could successfully predict lung delivery efficiency consistent with *in vivo* findings.

More recently, complete-airway simulations have been used to better understand respiratory drug delivery from commercial inhalers and to make new discoveries. This approach was first illustrated by Tian et al. [55] with the Flovent Diskus DPI delivering fluticasone propionate. In Tian et al. [55] and subsequent complete-airway studies, concurrent analysis was key in which realistic *in vitro* deposition experiments were used to measure the initial aerosol size emitted from the device and to benchmark regional aerosol deposition in the upper airways. The study of Tian et al. [55] illustrated the prediction of regional aerosol

deposition in the mouth-throat and in regional airway sections corresponding to the upper tracheobronchial (TB) airways (trachea to B3), mid-level TB airways (B4–B7), lower TB airways (B8–B15) and the alveolar region. An advantage of the CFD model results compared with *in vivo* studies using 2D gamma scintigraphy or 3D SPECT imaging is that regional deposition can be predicted directly and does not require translation from 2D images or 3D shells. The simulations correctly matched *in vitro* results for different inhalation profiles, supporting the idea that DPI testing should be conducted with realistic inhalation breath profiles for some inhalers [79].

In a subsequent study, Longest et al. [13] applied a complete-airway model to make a head-to-head comparison between a commercial MDI and a commercial DPI, each delivering the same drug (fluticasone propionate) and the same nominal drug dose. Using the patient information leaflet recommended inhalation flow profile, the MDI was predicted to deliver approximately 8.1% of the inhaled dose to the TB region and 51.9% to the alveolar airways. For the DPI, delivery fractions were cut in half with 4.2% depositing in the TB region and 26.1% depositing in the alveolar airways. Hence, both devices delivered nearly equal ratios for the TB : alveolar dose. Frequently, inhalation errors are cited as a reason for a preference to use DPIs, which are typically less efficient at lung delivery, compared with MDIs. However, the study of Longest et al. [13] showed that for at least one common significant inhalation error (inhalation flow rate), both inhalers were affected equally.

A potentially significant finding of complete-airway models is the relatively low drug dose that is delivered to the small TB airways. For commonly used MDIs and DPIs, several complete-airway studies reveal that the deposition fraction in the entire lower TB region is <1% of the total inhaled drug [13, 28]. When this area is refined further to include TB airways with a diameter of 2 mm or smaller, the deposited dose goes even lower to a value of approximately 0.4% of the inhaled drug [95]. Walenga and Longest [95] pointed out that this approximately 1 μg dose is spread over a small TB airway surface area of approximately 2,000 cm^2 when inhaling a nominal dose of 250 μg. Furthermore, the relative surface concentration of drug, assuming similar dissolution in each lung region, is three orders of magnitude lower in the small TB airways compared to the mouth-throat region. It has yet to be determined if these very low surface concentrations in the small airways can have an anti-inflammatory effect and if they can quantitatively explain the observation of persistent inflammation that occurs in the lower lungs with asthma in many cases [4, 123, 124].

6. Development of new respiratory drug delivery strategies

Concurrent CFD and *in vitro* experimental analysis have been important tools in the development of new respiratory drug delivery strategies. The first newly proposed aerosol delivery strategy based on CFD simulations was developed by Kleinstreuer et al. [63]. This study suggested controlling the spatial release position of orally inhaled medications to target delivery within different regions of the lungs. Provided that inhalation is slow enough to maintain laminar conditions through the glottis, Kleinstreuer et al. [63] demonstrated control of the aerosol through the lobar bronchi. The use of magnetically targeted aerosols has also been evaluated using CFD studies [125]. However, CFD results for magnetic

aerosols presented by Xie et al. [126, 127] highlight that the required magnetic forces may be difficult to achieve on the spatial scale of human lungs.

A new aerosol targeting strategy referred to as controlled condensational growth has been largely developed based on concurrent CFD and realistic *in vitro* experimental analysis. With controlled condensational growth relatively small particles or droplets are inhaled to minimize extrathoracic depositional losses. Due to the small size of the aerosol, the individual particles or droplets would ordinarily lack the mass and momentum required for deposition in the airways and would be exhaled. However, with controlled condensational growth, different approaches are used to increase the size of the aerosol particles or droplets once inside the airways. Using the enhanced condensational growth (ECG) method, the submicrometer-sized aerosol is inhaled with a separate stream of saturated air that is a few degrees above body temperature [94, 128, 129]. Mixing the aerosol and water vapor streams and cooling to body temperature produces supersaturated conditions and rapid increase in aerosol size for any aerosol. Excipient enhanced growth (EEG) is a second condensational growth approach in which individual particles or droplets contain both the medication and hygroscopic excipient as an engineered submicrometer formulation [130, 131]. Once inside the airways, the hygroscopic excipient takes up water, due to the natural high humidity of the lungs, causing size increase and allowing for targeted lung deposition. With both ECG and EEG, the rate of size increase can be controlled with various input parameters, such as inhaled inlet temperature or amount of hygroscopic excipient, and the effects of these parameters can be analyzed and optimized with CFD simulations.

Considering controlled condensational growth, key findings from CFD and concurrent realistic *in vitro* experimental analysis include <1% mouth-throat depositional loss. For example, with ECG delivery of a nebulized aerosol produced using a novel mixer-heater system, total mouth-throat depositional loss was illustrated to be <1% and significant aerosol size increase was observed as the aerosol exited approximately the third respiratory bifurcation [128]. Longest et al. [132] considered a soft mist inhaler formulated to deliver a submicrometer EEG aerosol using CFD simulations and *in vitro* experimental analysis. Both the model and experiments indicated that mouth-throat depositional loss was less than 1% in a representative extrathoracic airway geometry. Due to the inclusion of the hygroscopic excipient, the geometric aerosol size after a time period consistent with inhalation, was approximately 2.8 to 4.6 μm, which is consistent with the initial sizes used in conventional respiratory drug delivery [132]. In comparison with conventional inhalers, which produce mouth-throat deposition of 25–75%, the controlled condensational growth technique was demonstrated to reduce extrathoracic depositional loss by 1 to 2 orders of magnitude and could be adapted for use with handheld DPIs, SMIs or nebulizers [128, 132]. The complete-airway study of Tian et al. [133] indicated that EEG particles could attain diameters as large as ~5 μm entering the alveolar region. Moreover, EEG delivery could increase the small TB airway fraction by a factor of 40 compared with conventional inhalers, based on consistent complete-airway simulations [133].

A second aerosol delivery strategy that is being optimized with CFD simulations and concurrent *in vitro* experiments is nose-to-lung (N2L) or trans-nasal aerosol delivery with a nasal cannula interface. Longest et al. [134] considered conventional size aerosols (4–5 μm)

delivered through a high-flow nasal cannula (HFNC) patient interface at adult flow rates in the range of 30 to 45 L/min which is recognized to have very poor drug aerosol delivery efficiencies. The development of new streamlined connections and nasal cannula interface with CFD improved aerosol delivery efficiency through the system by factors of approximately 2 to 3. For a 4 μm aerosol delivered at 30 L/min with a streamlined nasal cannula interface, the system emitted dose was approximately 50% of the nebulized dose [134]. However, additional depositional losses are expected in the nasal extrathoracic airways.

To further maximize lung delivery efficiency and potentially enable the targeted delivery of pharmaceutical aerosols, trans-nasal aerosol administration has been coupled with controlled condensational growth and evaluated using concurrent CFD simulations and *in vitro* experiments. In an initial proof of concept study, ECG N2L delivery was evaluated in which a submicrometer aerosol was administered through one nostril and a saturated airstream was delivered through the other nostril [135]. CFD predictions indicated that nasal depositional loss was minimal (~5%) and that significant aerosol growth was achieved as the aerosol entered the lungs [135]. A CFD study by Walenga et al. [136] considered variability in N2L aerosol administration across four different nasal models that represented a wide range of expected depositional loss. For conventional size aerosols, in the range of 5 μm, deposition in the nasal airway ranged from 16 – 66%, whereas for EEG delivery, nasal depositional loss was only 2.3 – 3.1% [136]. Hence, EEG N2L delivery produced low inter-subject variability in the lung penetration of drug. In a series of studies, our group has also used concurrent analysis to optimize EEG N2L aerosol delivery with nasal cannula interfaces and cyclic breathing conditions for adult airway models [137, 138, 139, 140]. Concurrent analysis has also been used to demonstrate high efficiency lung delivery of EEG powder-based aerosol through nasal cannula [141] and facemask [142] interfaces.

7. Application of deposition modeling in challenging aerosol delivery scenarios

7.1 Pharmaceutical aerosol delivery to infants and children

The delivery of aerosolized medications to infants and children is known to be very inefficient with high intersubject variability [143, 144, 145]. A number of studies have highlighted challenges associated with pediatric aerosol delivery including low delivery efficiency in combination with very poor cooperation of the infant or pediatric subject in receiving the medication [146, 147, 148]. Benchtop realistic *in vitro* airway models with realistic inhalation conditions have frequently been used to better understand aerosol delivery to pediatric subjects and to improve delivery strategies [149, 150]. In contrast, CFD has been used only on limited basis, despite being well suited for applications in which human subjects testing is exceedingly difficult. A recent review by Carrigy et al. [151] addressed many aspects of CFD applied to simulating aerosol delivery to pediatric subjects. In the section below, we review highlights of CFD applied to respiratory drug delivery for infants and children organized based on CFD contributions in the areas of general observations, device development, and evaluation of new delivery strategies.

Considering general observations, studies by Xi and co-workers have evaluated the nasal deposition fraction of aerosols inhaled without a patient interface [152, 153, 154]. Infants are obligate nasal breathers, so nasal delivery efficiency provides valuable information about potential trans-nasal aerosol delivery when the aerosol is administered via a mask interface. These CFD studies highlight high nasal depositional loss and very low lung delivery efficiency that is achieved with the inhalation of conventional aerosol sizes in the range of 3 to 6 μm [154]. For example, the inhalation of a 5 μm droplet by a 5-year-old child at a typical flow rate of 20 L/min results in 80% nasal depositional loss of the aerosol [154]. Inhalation of an ultrafine aerosol in the range of 100 nm produces very low nasal depositional loss [152], but the aerosol will be largely exhaled from the lungs, as shown by Xi and Longest [155]. Xi et al. [153] illustrated that a 2.5 μm aerosol has overall <20% nasal depositional loss across a range of subject ages from 10 days old through adult, for one subject in each age range. This may indicate a better starting point for particle size to improve the efficiency of trans-nasal aerosol delivery at all ages.

Devices intended to improve respiratory drug delivery to pediatric subjects that have been analyzed or developed via CFD include an aerosol administration hood [156] and streamlined Y-connector [157] for use in mechanical ventilation. Shakked et al. [156] applied CFD modeling to evaluate the amount of nebulized aerosol that reached the nostrils of an infant when administered with a hood apparatus containing a delivery tube. CFD simulations indicated that when the tube was positioned directly over and within ~1 cm of the infant nostrils, approximately 18% of the released aerosol could enter the nose. However, a 10° angle of the delivery tube or a 10° rotation of the infant's head reduced nostril inhalation efficiency by factors as high as 5-fold. As illustrated by Xi and coworkers [154], additional depositional loss in the infant nasal airways may be substantial. The significant variability in nasal delivery efficiency observed by Shakked et al. [156] further illustrates why blow-by aerosol delivery, where the nebulizer is simply held close to the infant's nose, is not recommended [146, 148].

For infants receiving invasive mechanical ventilation with an endotracheal tube (ETT), Longest et al. [157] developed a streamlined Y-connector (joining inspiratory and expiratory lines with the ETT) and sought optimal conditions for the administration of conventional-sized nebulized droplets. Delivery conditions were consistent with a full-term infant and a 3 mm (internal diameter) curved ETT. Based on CFD simulations with cyclic ventilation, the streamlined Y-connector design reduced depositional losses in the connector by factors of approximately 2–4 and improved lung delivery efficiencies by a factor of approximately 2 compared with the commercial non-streamlined Y-connector. Delivery of the aerosol over the first half of the inspiratory cycle reduced exhaled dose from the ventilation circuit by a factor of 4 compared with continuous delivery. Optimal lung deposition was achieved with the streamlined Y-connector and breath synchronized delivery resulting in 45% and 60% lung deposition for optimal polydisperse (~1.78 μm) and monodisperse (~2.5 μm) particle sizes, respectively. Optimization of selected factors and use of the new Y-connector was shown to substantially increase the predicted lung delivery efficiency of medical aerosols to infants from current values of <1–10% to a range of 45–60%.

Considering the development of new aerosol delivery strategies with CFD, Longest and Tian [158] evaluated application of the EEG approach to a 6-month-old complete-airway infant model receiving mechanical ventilation with a 4 mm (internal diameter) ETT. Conventional aerosol delivery consisted of a mesh nebulizer positioned in the inspiratory arm of the ventilator circuit delivering an aerosol with a mass median aerodynamic (MMAD) diameter of 4.9 μm. With EEG delivery, two new streamlined Y-connectors were considered in which the aerosol was either administered upstream or administered in a port aligned with the ETT inlet. The EEG aerosol had a MMAD of approximately 0.9 μm and consisted of a model drug and NaCl as the hygroscopic excipient. CFD simulations indicated a size increase of the hygroscopic aerosol to approximately 5 μm in the mid- tracheobronchial airways. Compared to the commercial device and nebulized aerosol, the EEG approach with an initial 0.9 μm aerosol combined with the streamlined and streamlined-port geometries reduced device depositional losses by factors of 3-fold and >10-fold, respectively. With EEG powder aerosols, the streamlined geometry provided the maximum tracheobronchial deposition fraction (55.7%), whereas the streamlined-port geometry provided the maximum alveolar (67.6%) and total lung (95.7%) deposition fractions, respectively. Provided the aerosol could be administered in the first portion of the inspiration cycle, the proposed new method was predicted to significantly improve the deposition of pharmaceutical aerosols in the lungs of intubated infants.

7.2 Aerosol delivery to diseased lungs

CFD models have evaluated respiratory flow and aerosol deposition in several lung and lung-related diseases, including asthma, bronchial tumors, chronic obstructive pulmonary disease (COPD), and cystic fibrosis (CF). Studies involving asthmatic lungs consider the effects of bronchodilator delivery with luminal wall narrowing throughout the entire lung as would occur with long term airway remodeling [95, 122, 159, 160, 161, 162], or acute bronchoconstriction during an asthma attack [163, 164]. A few studies have also evaluated flow fields and particle trajectories in bronchi with tumors [165, 166, 167, 168]. In this section we focus primarily on studies addressing COPD and CF.

De Backer and co-workers have developed a method called Functional Respiratory Imaging (FRI) to measure the effect of bronchodilators in a number of studies [169, 170, 171], whereby model geometry is developed from computed tomography (CT) scans of patients with COPD, and used with CFD to determine airway volumes and resistance. Recent airway models for rats [172] and humans [173] explore the effect of boundary conditions in great detail by comparing the effect of healthy and diseased distal flow rates applied to the outlets of upper-airway geometries from CT scans.

A new and emerging application of CFD is the prediction of aerosol deposition for the respiratory delivery of antibiotics used to treat bacterial infections associated with CF (particularly *Pseudomonas aeruginosa*). The first CFD study of CF lungs, conducted by Awadalla et al. [174], was a porcine model of CF that replicated CF in the human lung with the same genetic defect. Their geometries were developed by segmentation of CT scans from five healthy and five CF model newborn pigs, and flow solutions with particle tracking were obtained using an in-house Large Eddy Simulation (LES) code. Results show that the

CF lungs gave a higher pressure drop, flow velocity, and resistance, due to smaller diameter airways. The differences in lung structure between healthy and CF lungs also demonstrated variations in flow and aerosol deposition patterns, but there was also inter-subject variability within each group. They concluded that submicrometer particle sizes may be required to treat the narrower airways that are present in CF lungs. Soon after this study, Bos et al. [175] published the first CFD study on human CF lungs, with the primary objective of determining whether current doses of the antibiotic aztreonam lysine (AZLI) provide sufficient concentrations in the airway surface liquid. Models were developed using CT scans from 40 children (5–17 years) and CFD simulations were run under transient conditions with LES turbulence models and Runge-Kutta particle tracking. An interesting finding from this study was that the more diseased lung lobes received less drug than healthier lobes. However, in the majority of cases considered, the concentration of AZLI in the airway surface liquid was deemed sufficient to treat the infection. One limitation of this study was that the CFD deposition data was not directly validated against *in vitro* or *in vivo* results, though predicted concentrations in the central airways were similar to sputum concentrations from clinical studies. Bos et al. extended this study and evaluated once- or twice-daily dosing of inhaled tobramycin from two different nebulizer platforms [57]. Twelve models (from the original set of 40 subjects) were chosen, with ages between 12–17 years, and results showed that the Akita nebulizer was twice as efficient as the PARI-LC in terms of lung delivery efficiency. They also concluded that the once daily, double dose of tobramycin would be more effective at killing bacteria and was expected to be safe compared to twice daily dosing, though further clinical testing was required.

8. Links to PK modeling and post-deposition transport

An important step in developing an inhaled medication is evaluating the pharmacokinetic (PK) distribution of drug throughout the body. Traditionally, this has been modeled with 1D or further simplified lung deposition predictions linked to PK or physiologically based (PB) pharmacokinetic models. However, research efforts are in progress to link CFD, or other mechanistic deposition models, with mechanistic simulations of dissolution, absorption and clearance, followed by traditional PK or PB-PK models to give a more accurate prediction of drug concentrations throughout the body [176, 177]. Linking CFD predictions of nasal uptake with a PK model of drug distribution was initially performed for tissue uptake of toxic gases [178]. Our group has proposed a complete nasal airway transport model to investigate the relationship between nasal spray drug deposition location in the nasal cavity and plasma drug concentrations [177, 179, 180], as illustrated in Figure 4. Realistic *in vitro* tests using a nasal airway model were first used to determine spray characteristics and validate local deposition within the nasal cavity. The new transport model implemented these deposition profiles as the suspended drug particle (mometasone furoate) starting locations for subsequent modeling of dissolution, absorption, and clearance in a nasal surface geometry [179, 180]. Once absorbed into the respiratory epithelium, a PK model was used to predict the drug plasma concentration profiles. The model predictions were validated using *in vivo* data for both nasal clearance rates and drug plasma concentration curves [177]. The model was then used to demonstrate a direct association between maximum blood concentration of drug (C_{max}) and middle passage nasal deposition of the model drug.

However, both middle passage deposition and C_{max} were shown to be highly sensitive to changes in patient-use parameters, such as spray nozzle insertion angle, nasal inhalation, and nose blowing, which could make the establishment of bioequivalence problematic [177]. As an alternative approach, it was suggested that a small PK (or radiological imaging) study be used to first validate a combination *in vitro-in silico* approach and this new combination method be used for establishing the local delivery component of bioequivalence testing [181].

9. Expert opinion

The development of complete-airway lung models represents a major advancement in the application of CFD to respiratory drug delivery. With these models, reasonably accurate predictions of how an inhaled drug distributes from the inhaler through the alveoli can be captured without the need for correction factors associated with multiple aspects of pharmaceutical aerosols [97, 98]. While relatively new, this approach is yielding interesting and compelling findings about existing inhalers and delivery strategies. For example, a comparison of MDI and DPI devices illustrated that a specific inhalation error, inappropriate flow rate, caused a similar decrease in tracheobronchial drug delivery for both inhalers [13]. In a side-by-side comparison, the DPI delivered the largest dose to the MT (~70%) and the MDI delivered the largest dose to the alveolar airways (~50%). In both cases, less than 1% of the aerosol dose deposited in the small tracheobronchial airways, which may be associated with the poor efficiency of inhaled corticosteroids in this area [5]. A comparison of the Respimat SMI and Novolizer DPI devices revealed that the Respimat device increased drug delivery efficiency to the small tracheobronchial areas by a factor of 10 [28]. However, total delivery efficiency to this important region remained less than 10% of the inhaled dose, resulting in surface concentrations of drug that were still significantly less than occur in the upper lung airways. Considering inhaled antibiotic delivery and a CFD model that included a majority of the tracheobronchial airways, Bos et al. [175] demonstrated how diseased airways lead to suboptimal antibiotic concentrations below the minimum inhibitory concentration (MIC) value. Considering small tracheobronchial airway deposition a step further, Walenga and Longest [95] reported that dose concentrations in this region are up to two orders of magnitude below concentrations in the upper airways for an MDI and DPI aerosol. Future studies are needed to determine if these drug concentration levels (in the range of 10^{-4} μg/cm^2) can effectively treat inflammation in models of asthmatic lung cells. However, these results provide support to the current theory that the small airways are frequently undertreated with inhaled corticosteroid therapy in asthma, potentially leading to uncontrolled small airway disease and non-responsive asthma [4, 5, 123, 124, 182, 183].

In the evaluation of aerosol deposition for respiratory drug delivery, the importance of frequent model validations with experiments and, when possible, concurrent *in vitro* and CFD analysis should be a top priority. A growing dataset of *in vitro* deposition case studies for commercial inhalers is available from our lab and others [11, 12, 13, 27, 28, 55, 80, 184]. As described, we have validated complete-airway simulations of DPI and SMI lung deposition on a regional basis with 2D gamma scintigraphy studies conducted in healthy human subjects [97, 98]. However, it was concurrent *in vitro* and CFD analysis that made development of the complete-airway CFD model possible [13, 28, 55]. In this approach, *in*

vitro experiments are used to determine initial aerosol size distributions, benchmark upper airway deposition data, and evaluate other factors such as particle size distributions exiting the airway model and aerosol size change. As a first step, the CFD model is validated with the *in vitro* data, preferably for multiple cases that may include multiple geometries or regions. Once validated, insights from the CFD simulations related to the aerosol transport and deposition are then valuable for understanding the *in vitro* results and behavior of the drug delivery system or device. The validated CFD model is then available to test and optimize different device designs such as altering dilution airflow inlet positions or their size to vary the aerosol spray properties. The recommended CFD design or strategy should then be verified with additional *in vitro* results, as illustrated with Hindle and Longest [83]. Our group has applied this concurrent analysis for the evaluation of existing devices [27], the development of new inhalers [82, 185, 186, 187], and the development of new respiratory drug delivery strategies [132, 141]. As CFD codes advance, once the model is created and validated, optimization routines including neural networks and artificial intelligence can be implemented to decrease analysis time and to further improve outcomes.

While useful, it should be noted that *in vitro* data supporting CFD simulations is difficult to obtain requiring specialized methods that are often not part of typical pharmaceutical aerosol testing protocols. For example, spray aerosols evolve rapidly in the vicinity of the inhaler and potentially in the MT region. Accurately measuring an initial size distribution of an evolving spray aerosol is challenging and may be achieved with laser diffraction systems [2, 27, 82]. The assessment of aerosol size distribution exiting the MT during realistic inhalation requires a specialized breath simulation system [79, 188]. Simple quantification methods such as HPLC may not be available for all medications, and labeling an aerosol with a quantifiable marker may change its size distribution or behavior. Continuing development and refinement of *in vitro* techniques for concurrent analysis is required in order to further improve the accuracy of CFD models. However, agreement between CFD predictions and *in vitro* results of regional and local aerosol deposition provides confidence that both techniques are being used effectively.

An important outcome of concurrent *in vitro* and CFD analysis as well as the use of complete-airway CFD models has been the development of new respiratory drug delivery strategies. As reviewed, both nose-to-lung delivery [136, 137, 141] and controlled condensational growth [128, 130, 133, 189] represent potentially important techniques that can dramatically improve aerosol lung delivery efficiency and target aerosolized medications within the lungs. Considering controlled condensational growth, initial concurrent analyses demonstrated that significant hygroscopic size increase was possible on the time scale of inhalation cycles for adults and children [129, 131, 189]. Concurrent analysis in regional models demonstrated that ~1% MT depositional loss could be achieved with ~99% lung delivery efficiency [128, 132]. Additional concurrent analysis has focused on developing aerosol generation and delivery devices [139, 185, 186, 187, 190].

Complete-airway simulations of N2L and oral inhalation delivery have demonstrated the potential for targeting drug deposition within lung regions, which will only be possible with high efficiency delivery methodologies [133, 191]. Based on this progression, a project is currently underway to test condensational growth aerosol delivery in human subjects using

2D gamma scintigraphy analysis. If successful, the controlled condensational growth strategy will represent the first significant improvement in respiratory drug delivery to arise from concurrent *in vitro* and CFD simulations including complete-airway CFD modeling.

A common question in the assessment and development of pulmonary products is what type of deposition model is sufficient. As described, 1D models are typically based on algebraic correlations and can be run on any current processor in a matter of seconds. In contrast, CFD models are based on first principles (fundamental conservation equations) and require many more input decisions, thorough training in CFD techniques, and considerable computational expense. Longest [192] recently addressed the question of model selection with comparisons of 1D, regional CFD, 3D/1D hybrid and complete-airway CFD models. In summary, this analysis emphasized that model selection depends on (i) complexity of the transport physics, (ii) availability and quality of the deposition correlations, and (iii) level of required detail in the output data. For simple low momentum aerosol delivery with wide mouthpieces, 1D models exhibit approximately 50–60% relative errors in comparison with *in vivo* data in the MT and alveolar regions [192]. Finlay and coworkers have improved MT deposition estimates for DPI aerosols delivered with a narrow diameter tube [18, 65]. However, the MT corrections may not be accurate for DPIs with more complex MP designs [185, 186, 193] and similar correlations have not been developed for spray aerosols or to account for the effect of nebulizer and SMI mouthpieces. Furthermore, correcting the MT deposition in 1D models is not sufficient to correct alveolar deposition, and large differences from *in vivo* measurements are expected to remain in this region [192]. Complete-airway CFD model predictions are currently within approximately 10% of *in vivo* data divided across the inhaler and three airway regions for complex spray and DPI aerosols [97, 98, 192].

An unresolved component of the model selection question relates to the need for additional model validations and for continued model refinements. Complexities of model validation with *in vivo* data are well described in Conway et al. [23] and include the need for adequate model inputs as well as variability in the *in vivo* data associated with factors such as subject positioning and the *in vivo* data processing approach selected. We believe that next steps in complete-airway CFD model validation include comparisons with 3D SPECT/CT data for nebulizer [23] and inhaler [194] generated aerosols, comparisons with branch-averaged data in the upper airways [23], and inclusion of significant aerosol size change. Fundamentally, 1D models can be more easily adjusted (or corrected) to match *in vivo* deposition data. This is because 1D models are based on deposition correlations, which are less realistic compared with CFD simulations. In contrast, complete-airway CFD models are based on first principles and may require the inclusion of even more advanced physics to match *in vivo* deposition in 3D space. For example, motion of the tracheobronchial airways [195] and glottis [196] during inhalation may influence deposition patterns. As we have previously discussed [97], *a priori* model estimates are important for modeling benefits to be maximized, in which, once the model is developed concurrently with *in vitro* experiments, it should be able to capture *in vivo* data without further or case-specific adjustments. Due to the more realistic nature of CFD predictions and reliance on first principles versus algebraic correlations, we believe that CFD modeling will ultimately be shown to be capable of making accurate *a prior* estimates of *in vivo* deposition across a range of pharmaceutical aerosol products.

As a next step in CFD model development, CFD models are envisioned to be coupled with physiologically based pharmacokinetic (PB-PK) models. Such a joint model combination will provide regional lung tissue concentrations of drug and traditional pharmacokinetic metrics like maximum blood concentration of drug and area under the drug concentration curve. For example, the study of Rygg et al. [177] coupled direct 3D CFD simulations of dissolution, absorption and clearance (DAC) in a nasal model, developed in [179, 180], with a PB-PK model of tissue clearance and plasma concentration (Figure 4). The Gastroplus™ (SimulationsPlus Inc., Rochester, US) model described by Backman et al. [176] implements a 1D deposition model with mechanistic models for dissolution and absorption coupled with a whole-body PB-PK model. In both cases [176, 177], the PK model was capable of matching *in vivo* measurement points of drug concentration in the blood. In this manner, a union of CFD (or 1D deposition modeling) with PK modeling can be used for pharmaceutical formulation screening and development [176, 177]. However, our belief is that there may always be too many biological unknowns for this approach to accurately represent a population of subjects. Instead, it can be viewed as a single consistent platform with a defined set of PK parameters used to test the effect of different inhalation device and formulation combinations.

An important aspect of coupled CFD and PK modeling is where to switch from the 3D resolved CFD approach to mechanistic 1D models and/or PK rate equations. Based on the findings of Longest and Hindle [14], illustrated in Figure 5, we propose that CFD simulation all the way through epithelial cell absorption has important implications to bioavailability that cannot be captured with 1D approximations or PK rate equations. Therefore, when PK metrics such as plasma drug concentration are of interest, we recommend that the protocol implemented by Rygg et al. [177] be followed in which the PK model is applied after epithelial cell absorption occurs with a 3D or other mechanistic model. Once inside the lung tissue, we view a PK model as valuable for determining tissue clearance and the prediction of plasma concentrations and distribution of drug throughout the body. Our assessment is that without CFD predictions through absorption, potentially important metrics such as the percentage of cells absorbing drug above a predefined threshold [14] cannot be accurately predicted.

In order for a generic inhalation product to be approved, it must be shown to be bioequivalent with the innovator product [197]. In determining bioequivalence for locally acting drugs, the FDA is required to assess bioavailability using scientifically valid measurements to reflect the rate and extent to which the drug becomes available at the site of action. Ideally, the regulators would seek to establish that for the generic and innovator products there are (*i*) similar drug concentration and time course at the site of action and (*ii*) similar systemic PK profiles, both of which are challenging in a clinical setting using the products as intended for clinical use. It is currently an open question as to whether PK can accurately determine local drug concentration profiles in the nose or in the lungs due to the low concentrations employed for locally acting products and due to the possibility that drug depositing in multiple regions with the airways may result in similar PK curves despite regional deposition differences. Furthermore, selection of multiple arbitrary PK absorption and rate constants can be used to match a predicted particle deposition distribution in the airways with an experimentally determined PK curve from human subjects. Therefore, we

do not think that matching PK data with a combined CFD-PK model is adequate validation of the lung deposition conditions predicted by CFD results. Furthermore, adding a PK model to CFD results blurs the useful findings of CFD, which relate to the stated purpose of bioequivalence testing, i.e., similar drug concentrations and time course at the site of action. As an alternative, we propose that concurrent *in vitro* and complete-airway CFD deposition modeling can be used to establish similar local concentration profiles throughout the lungs. These deposition profiles may be extended to dissolution, absorption and clearance with mechanistic models to predict lung absorption and the percentage of cells receiving drug, as illustrated by Longest and Hindle [14]. The appropriate validation of this approach is likely 2D gamma scintigraphy or 3D SPECT analysis with radiolabeled aerosols in human subjects, combined with clinical efficacy studies if possible. The combination of simulating complete-airway deposition patterns together with similar regional lung absorption and similar cellular absorption percentages (i.e., microdosimetry) is logically sufficient to establish similar local drug concentrations between a generic and innovator inhaler.

Based on decades of experimental research, intersubject variability in airway deposition is known to be very large for healthy subjects and in cases of airway disease [198, 199, 200]. *In vitro* models have helped to quantify expected intersubject variability for orally inhaled pharmaceutical products [11, 12, 184, 201], and for nasally inhaled aerosols in pediatric and infant populations [33, 202, 203, 204]. While CFD is well suited to study intersubject variability and diseased airway effects, studies have been relatively infrequent. One exception is the study of Walenga et al. [136], which used validated CFD simulations to demonstrate that the nasal deposition 95% confidence interval across a population of adults could be reduced from 15.5–66.3% to a range of 2.3–3.1% by the use of a small particle aerosol in N2L aerosol delivery. As demonstrated in Walenga et al. [136], once the CFD model is validated, it can be directly applied to different subject anatomies and flow conditions provided that the underlying physics of the flow are not changed. We believe that intersubject variability and the inclusion of diseased airway conditions are critical to consider in the development of new pulmonary delivery strategies and pharmaceutical aerosol products.

While currently proving useful, a number of advances are needed to improve CFD deposition models. More theoretical work is needed to understand and integrate the complex hydrodynamic process of particle or droplet near-wall interactions leading to deposition, and how this process is affected by the laminar sublayer, particle charge and airway or model surface properties. Complete-airway simulations require advancements to implement improved models of heterogeneous lung ventilation [121, 205, 206] in health and disease, as well as exhalation and cyclic breathing. Chronic and short term geometrical changes associated with airway disease need to be further investigated. Simulations of post-deposition transport are in early stages of development. Backman [176] describes a number of unknowns required for accurate mechanistic models of post-deposition transport. Continued validation is needed for complete-airway predictions of commercial and next generation inhalers including multiple inhaler types, additional flow rates and extension to 3D imaging results. Improved mechanisms are needed to validate drug absorption into lung tissue beyond PK profiles. Some studies on lung permeability and drug absorption using multiple radiolabeled small-molecule probes are already available [207]. Experimental 3D

rendering of drug absorption, perhaps through PET scanning [207], would be desirable to validate complete-airway simulations coupled with epithelial uptake. As suggested by Corcoran [207], imaging techniques that predict pathophysiology of disease could be used to generate patient-specific maps of the airways with drug delivery tailored using co-localized imaging or complete-airway CFD predictions.

In summary, effective respiratory drug delivery is a highly complex undertaking from both a physical and biological perspective. CFD deposition models have made significant progress over the last 20 years in helping to understand the physics of respiratory drug delivery. With the development of complete-airway CFD deposition models, new insights are being made regarding current inhalers that support clinical hypotheses, such as the common under treatment of the small airways in asthma [123] or suboptimal antibiotic concentrations in diseased airways [175]. These complete-airway models are also being used to advance next generation delivery strategies, like controlled condensational growth, which are currently in development for human subjects testing. Considering application to bioequivalence testing, we recommend further evaluation of currently available metrics including regional lung deposition profiles, regional drug absorption fractions and percentages of cells receiving drug without the blurring of results associated with linking PK and deposition. We view the next frontier in CFD deposition modeling as 3D time-resolved dissolution, absorption and clearance (DAC) predictions, as presented in our recent work [14] and illustrated in Figure 5. As envisioned many years ago, microdosimetry patterns are most likely important for many surface active molecules and the capability to use these patterns in predicting bioavailability and concentration-related aspect of efficacy may be within reach.

Acknowledgments

Funding

The authors were supported by the Eunice Kennedy Shriver National Institute of Child Health & Human Development under Award Number R01HD087339 and by the National Heart, Lung, and Blood Institute under Award Numbers R01HL139673 and R01HL107333. The content is solely the responsibility of the authors and does not necessarily represent the official views of the National Institutes of Health.

References

Papers of special note have been highlighted as:

* of interest

** of considerable interest

1. Finlay WH. The Mechanics of Inhaled Pharmaceutical Aerosols. San Diego: Academic Press; 2001.**Explains the scientific principles of pharmaceutical aerosols
2. Longest PW, Hindle M, Das Choudhuri S, et al. Comparison of ambient and spray aerosol deposition in a standard induction port and more realistic mouth-throat geometry. J Aerosol Sci. 2008;39(7):572–591.
3. Usmani OS, Biddiscombe MF, Barnes PJ. Regional lung deposition and bronchodilator response as a function of beta(2)-agonist particle size. American Journal Of Respiratory And Critical Care Medicine. 2005 12 15;172(12):1497–1504. [PubMed: 16192448]
4. Usmani OS, Singh D, Spinola M, et al. The prevalence of small airways disease in adult asthma: A systematic literature review. Respiratory Medicine. 2016;116:19–27. [PubMed: 27296816]

5. Berry M, Hargadon B, Morgan A, et al. Alveolar nitric oxide in adults with asthma: evidence of distal lung inflammation in refractory asthma. The European respiratory journal. 2005;25(6):986–91. [PubMed: 15929952]

6. Weers J Inhaled antimicrobial therapy - Barriers to effective treatment. Advanced Drug Delivery Reviews. 2015;85:24–43. [PubMed: 25193067]

7. Geller DE. Aerosol antibiotics in cystic fibrosis. Respiratory Care. 2009;54(5):658–670. [PubMed: 19393109]

8. Willson DF. Aerosolized surfactants, anti-inflammatory drugs, and analgesics. Respiratory Care. 2015;60(6):774–793. [PubMed: 26070574]

9. Patton JS, Brain JD, Davies LA, et al. The particle has landed-Characterizing the fate of inhaled pharmaceuticals. J Aerosol Med Pulm Drug Deliv. 2010 12;23:S71–S87. [PubMed: 21133802]

10. Sakagami M In vivo, in vitro and ex vivo models to assess pulmonary absorption and disposition of inhaled therapeutics for systemic delivery. Advanced Drug Delivery Reviews. 2006;58:1030–1060. [PubMed: 17010473]

11. Delvadia R, Hindle M, Longest PW, et al. In vitro tests for aerosol deposition II: IVIVCs for different dry powder inhalers in normal adults. J Aerosol Med Pulm Drug Deliv. 2013;26(3):138–144. [PubMed: 22947131]

12. Wei X, Hindle M, Kaviratna A, et al. In Vitro Tests for Aerosol Deposition. VI: Realistic Testing with Different Mouth–Throat Models and In Vitro—In Vivo Correlations for a Dry Powder Inhaler, Metered Dose Inhaler, and Soft Mist Inhaler. J Aerosol Med Pulm Drug Deliv. 2018;10.1089/jamp.2018.1454.*Broad source of in vitro experimental data available for validating CFD models

13. Longest PW, Tian G, Walenga RL, et al. Comparing MDI and DPI aerosol deposition using in vitro experiments and a new stochastic individual path (SIP) model of the conducting airways. Pharmaceutical Research. 2012;29:1670–1688. [PubMed: 22290350]

14. Longest PW, Hindle M. Small airway absorption and microdosimetry of inhaled corticosteriod particles after deposition. Pharm Res. 2017;34(10):2049–2065. [PubMed: 28643237] * Uses CFD to illustrate that heterogeneous absorption of corticosteroids in small airways can be improved through the use of small particle aerosols

15. Arora D, Shah KA, Halquist MS, et al. In vitro aqueous fluid-capacity-limited dissolution testing of respirable aerosol drug particles generated from inhaler products. Pharmaceutical Research. 2010 5;27(5):786–795. [PubMed: 20229134]

16. Longest PW, Holbrook LT. In silico models of aerosol delivery to the respiratory tract - Development and applications. Advanced Drug Delivery Reviews. 2012;64:296–311. [PubMed: 21640772] *Review of CFD applied to respiratory drug delivery with a focus on regional deposition

17. Stahlhofen W, Rudolf G, James AC. Intercomparison of experimental regional aerosol deposition data. Journal of Aerosol Medicine. 1989;2(3):285–308.

18. Finlay WH, Martin AR. Recent advances in predictive understanding of respiratory tract deposition. J Aerosol Med Pulm Drug Deliv. 2008;21(2):189–205. [PubMed: 18518795] *Summarizes deposition correlations from in vivo, in vitro and CFD sources

19. Choi J, Kim CS. Mathematical analysis of particle deposition in human lungs: an improved single path transport model. Inhal Toxicol. 2007;19:925–939. [PubMed: 17849277]

20. Asgharian B, Hofmann W, Bergmann R. Particle deposition in a multiple-path model of the human lung. Aerosol Science and Technology. 2001;34:332–339.**Important study illustrating 1D deposition modeling using a random pathway approach

21. Martonen TB. Analytical model of hygroscopic particle behavior in human airways. Bulletin of Mathematical Biology. 1982;44(3):425–442. [PubMed: 7104512] **Classic exposition that describes complete-airway algebraic deposition models

22. Katz I, Pichelin M, Caillibotte G, et al. Controlled, parametric, individualized, 2D, and 3D imaging measurements of aerosol deposition in the respiratory tract of healthy human subjects: Preliminary comparisons with simulations. Aerosol Science and Technology. 2013 7;47(7):714–723. doi: 10.1080/02786826.2013.784393..**Recent assessment illustrating the limitations of 1D deposition modeling compared with in vivo deposition data

23. Conway J, Fleming J, Majoral C, et al. Controlled, parametric, individualized, 2-D and 3-D imaging measurements of aerosol deposition in the respiratory tract of healthy human subjects for model validation. J Aerosol Sci. 2012 10;52:1–17.**Provides valuable in vivo data for a low momentum nebulized aerosol that can be applied to validate complete-airway CFD predictions
24. Fleming JS, Epps BP, Conway JH, et al. Comparison of SPECT aerosol deposition data with a human respiratory tract model. Journal Of Aerosol Medicine-Deposition Clearance And Effects In The Lung. 2006 Fal;19(3):268–278.
25. Koblinger L, Hofmann W. Monte Carlo modeling of aerosol deposition in human lungs. Part I: Simulation of particle transport in a stochastic lung structure. J Aerosol Sci. 1990;21(5):661–674.
26. Kim CS. Deposition of aerosol particles in human lungs: in vivo measurement and modeling. Biomarkers. 2009;14(S1):54–58. [PubMed: 19604060]
27. Longest PW, Hindle M. Evaluation of the Respimat Soft Mist inhaler using a concurrent CFD and in vitro approach. J Aerosol Med Pulm Drug Deliv. 2009;22(2):99–112. [PubMed: 18956950]
28. Longest PW, Tian G, Delvadia R, et al. Development of a stochastic individual path (SIP) model for predicting the deposition of pharmaceutical aerosols: Effects of turbulence, polydisperse aerosol size, and evaluation of multiple lung lobes. Aerosol Science and Technology. 2012;46(12): 1271–1285.*Development and progression of a CFD complete-airway model
29. Oldham MJ, Phalen RF, Heistracher T. Computational fluid dynamic predictions and experimental results for particle deposition in an airway model. Aerosol Science and Technology. 2000 1;32(1): 61–71.*Provides valuable data to validate CFD deposition predictions on a mm-scale grid
30. Sznitman J, Sutter R, Altorfer D, et al. Visualization of respiratory flows from 3D reconstructed alveolar airsapces using X-ray tomographic microscopy. J Vis. 2010;13:337–345.
31. DeHaan WH, Finlay WH. Predicting extrathoracic deposition from dry powder inhalers. J Aerosol Sci. 2004;35:309–331.*Provides corrections to mouth-throat deposition that accounts for narrow diameter DPI mouthpieces
32. Xi J, Longest PW. Numerical predictions of submicrometer aerosol deposition in the nasal cavity using a novel drift flux approach. International Journal Of Heat And Mass Transfer. 2008;51:5562–5577.
33. Golshahi L, Noga ML, Finlay WH. Deposition of inhaled micrometer-sized particles in oropharyngeal airway replicas of children at constant flow rates. J Aerosol Sci. 2012;49:21–31.
34. Tannehill JC, Anderson DA, Pletcher RH. Computational Fluid Mechanics and Heat Transfer. 2 ed. Washington: Taylor and Francis; 1997.
35. Patankar S Numerical Heat Transfer and Fluid Flow. CRC press; 1980.
36. Balashazy I, Hofmann W. Particle deposition in airway bifurcations-II. Expiratory flow. J Aerosol Sci. 1993;24:773–786.
37. Finlay W, Stapleton K, Yokota J. On the use of computational fluid dynamics for simulating flow and particle deposition in the human respiratory tract. Journal of Aerosol Medicine. 1996;9(3): 329–341.*Reviewed some of the first applications of CFD to predict particle deposition in the airways
38. Kimbell JS, Gross EA, Joyner DR, et al. Application of computational fluid dynamics regional dosimetry of inhaled chemicals in the upper respiratory tract of the rat. Toxicol Appl Pharmacol. 1993;121:253–263. [PubMed: 8346542]
39. Comer JK, Kleinstreuer C, Hyun S, et al. Aerosol transport and deposition in sequentially bifurcating airways. Journal of Biomechanical Engineering. 2000 4;122(2):152–158. [PubMed: 10834155]
40. Martonen TB, Guan XF. Effects of tumors on inhaled pharmacologic drugs II. Particle motion. Cell Biochemistry And Biophysics. 2001;35(3):245–253. [PubMed: 11894844]
41. Xi J, Longest PW, Martonen TB. Effects of the laryngeal jet on nano- and microparticle transport and deposition in an approximate model of the upper tracheobronchial airways. Journal of Applied Physiology. 2008;104(6):1761–1777. [PubMed: 18388247]
42. Longest PW, Vinchurkar S, Martonen TB. Transport and deposition of respiratory aerosols in models of childhood asthma. J Aerosol Sci. 2006;37:1234–1257.*Highlighted the effect of airway constriction on particle hotspot formation

43. Sznitman J, Heimshch T, Wildhaber JH, et al. Respiratory flow phenomena and gravitational deposition in a three-dimensional space-filling model of the pulmonary acinar tree. Journal of Biomechanical Engineering. 2009;131:031010–1–15. [PubMed: 19154069] *Highly realistic CFD model of the acinar region
44. Lambert AR, O'Shaughnessy PT, Tawhai MH, et al. Regional deposition of particles in an image-based airway model: Large-eddy simulation and left-right lung ventilation asymmetry. Aerosol Science and Technology. 2011;45:11–25. [PubMed: 21307962] **Excellent use of CFD to illustrate physiological phenomena
45. Inthavong K, Choi L-T, Tu J, et al. Micron particle deposition in a tracheobronchial airway model under different breathing conditions. Medical Engineering and Physics. 2010;32:1198–1212. [PubMed: 20855226]
46. Lin C-L, Tawhai MH, McLennan G, et al. Characteristics of the turbulent laryngeal jet and its effect on airflow in the human intra-thoracic airways. Respiratory Physiology and Neurobiology. 2007;157:295–309. [PubMed: 17360247]
47. Choi J, Tawhai M, Hoffman EA, et al. On intra- and intersubject variabilities of airflow in the human lungs. Physics of Fluids. 2009;21:101901–1–17. [PubMed: 19901999]
48. Li Z, Kleinstreuer C, Zhang Z. Particle deposition in the human tracheobronchial airways due to transient inspiratory flow patterns. Aerosol Science. 2007;38:625–644.
49. Cui Y, Sommerfeld M. Forces on micron-sized particles randomly distributed on the surface of larger particles and possibility of detachment. International Journal of Multiphase Flow. 2015;72:39–52.
50. Cui Y, Sommerfeld M. Application of lattice-Boltzmann method for analysing detachment of micron-sized particles from carrier particles in turbulent flows. Flow, Turbulence and Combustion. 2018;100(1):271–297.
51. Sommerfeld M, Schmalfuß S. Numerical analysis of carrier particle motion in a dry powder inhaler. Journal of Fluids Engineering. 2016;138(4):041308.
52. Wong W, Fletcher DF, Traini D, et al. The use of computational approaches in inhaler development. Advanced Drug Delivery Reviews. 2012 3 30;64(4):312–322. [PubMed: 22063020] *Reviews CFD applied to inhaler development
53. Ruzycki CA, Javaheri E, Finlay WH. The use of computational fluid dynamics in inhaler design. Expert opinion on drug delivery. 2013;10(3):307–323. [PubMed: 23289401] *Reviews CFD applied to inhaler design
54. Matida EA, Finlay WH, Breuer M, et al. Improving prediction of aerosol deposition in an idealized mouth using large-eddy simulation. Journal of Aerosol Medicine. 2006;19(3):290–300. [PubMed: 17034305]
55. Tian G, Longest PW, Su G, et al. Development of a stochastic individual path (SIP) model for predicting the tracheobronchial deposition of pharmaceutical aerosols: Effects of transient inhalation and sampling the airways. J Aerosol Sci. 2011;42:781–799.*Development and progression of a CFD complete-airway model
56. Khajeh-Hosseini-Dalasm N, Longest PW. Deposition of particles in the alveolar airways: Inhalation and breath-hold with pharmaceutical aerosols. J Aerosol Sci. 2015;79:15–30. [PubMed: 25382867] *Illustrates the developed and CFD simulation of a realistic complete acinar unit geometry
57. Bos AC, Mouton JW, van Westreenen M, et al. Patient-specific modelling of regional tobramycin concentration levels in airways of patients with cystic fibrosis: can we dose once daily? [Article]. J Antimicrob Chemother. 2017 12;72(12):3435–3442. doi: 10.1093/jac/dkx293. English. [PubMed: 29029057]
58. Lin CL, Tawhai MH, Hoffman EA. Multiscale image-based modeling and simulation of gas flow and particle transport in the human lungs. Wiley Interdiscip Rev Syst Biol Med. 2013 Sep-Oct; 5(5):643–55. doi: 10.1002/wsbm.1234. [PubMed: 23843310]
59. Zhang Z, Kleinstreuer C, Kim CS. Airflow and nanoparticle deposition in a 16-generation tracheobronchial airway model. Ann Biomed Eng. 2008;36(12):2095–2110. [PubMed: 18850271]
60. Gemci T, Ponyavin V, Chen Y, et al. Computational model of airflow in upper 17 generations of human respiratory tract. J Biomech. 2008;41(9):2047–2054. [PubMed: 18501360]

61. Kleinstreuer C, Zhang Z, Li Z. Modeling airflow and particle transport/deposition in pulmonary airways. Respiratory Physiology and Neurobiology. 2008;163:128–138. [PubMed: 18674643]
62. Zhang Z, Kleinstreuer C, Donohue JF, et al. Comparison of micro- and nano-size particle depositions in a human upper airway model. J Aerosol Sci. 2005 2;36(2):211–233.
63. Kleinstreuer C, Shi H, Zhang Z. Computational analyses of a pressurized metered dose inhaler and an new drug-aerosol targeting methodology. Journal of Aerosol Medicine. 2007;20(3):294–309. [PubMed: 17894536] *First study to accurately model deposition from an MDI in the mouth-throat; and first study to use CFD to demonstrate a method for controlling aerosol transport within the lungs
64. Ilie M, Matida EA, Finlay WH. Asymmetrical aerosol deposition in an idealized mouth with a DPI mouthpiece inlet. Aerosol Science and Technology. 2008;42:10–17.
65. Finlay WH, Martin AR. Modeling of aerosol deposition within interface devices. Journal of Aerosol Medicine. 2007;20(S1):S19–S28. [PubMed: 17411402]
66. Katz IM, Davis BM, Martonen TB. A numerical study of particle motion within the human larynx and trachea. J Aerosol Sci. 1999 2;30(2):173–183.
67. Miyawaki S, Tawhai MH, Hoffman EA, et al. Effect of carrier gas properties on aerosol distribution in a CT-based human airway numerical model. Ann Biomed Eng. 2012;40(7):1495–1507. [PubMed: 22246469]
68. Miyawaki S, Hoffman EA, Lin C-L. Numerical simulations of aerosol delivery to the human lung with an idealized laryngeal model, image-based airway model, and automatic meshing algorithm. Computers & fluids. 2017;148:1–9. [PubMed: 28959080]
69. Sznitman J, Heimsch F, Heimsch T, et al. Three-dimensional convective alveolar flow induced by rythmic breathing motion of the pulmonary acinus. ASME Journal of Biomechanical Engineering. 2007;129:658–665.
70. Hofemeier P, Sznitman J. Revisiting pulmonary acinar particle transport: convection, sedimentation, diffusion, and their interplay. Journal of Applied Physiology. 2015;118(11):1375–1385. [PubMed: 25882387]
71. Oakes JM, Hofemeier P, Vignon-Clementel IE, et al. Aerosols in healthy and emphysematous in silico pulmonary acinar rat models. J Biomech. 2016;49(11):2213–2220. [PubMed: 26726781]
72. Ostrovski Y, Hofemeier P, Sznitman J. Augmenting regional and targeted delivery in the pulmonary acinus using magnetic particles. International journal of nanomedicine. 2016;11:3385. [PubMed: 27547034]
73. Hofemeier P, Koshiyama K, Wada S, et al. One (sub-) acinus for all: Fate of inhaled aerosols in heterogeneous pulmonary acinar structures. European Journal of Pharmaceutical Sciences. 2018;113:53–63. [PubMed: 28954217]
74. Koshiyama K, Wada S. Mathematical model of a heterogeneous pulmonary acinus structure. Comput Biol Med. 2015;62:25–32. [PubMed: 25912985]
75. Talaat K, Xi J. Computational modeling of aerosol transport, dispersion, and deposition in rhythmically expanding and contracting terminal alveoli. J Aerosol Sci. 2017;112:19–33.
76. Xi J, Talaat K, Si XA. Deposition of bolus and continuously inhaled aerosols in rhythmically moving terminal alveoli. The Journal of Computational Multiphase Flows. 2018:1757482X18791891.
77. Sera T, Higashi R, Naito H, et al. Distribution of nanoparticle depositions after a single breathing in a murine pulmonary acinus model. International Journal of Heat and Mass Transfer. 2017;108:730–739.
78. Roshchenko A, Minev PD, Finlay WH. A time splitting fictitious domain algorithm for fluid–structure interaction problems (A fictitious domain algorithm for FSI). Journal of Fluids and Structures. 2015;58:109–126.
79. Delvadia RR, Wei X, Longest PW, et al. In vitro tests for aerosol deposition. IV: Simulating variations in human breath profiles for realistic DPI testing. J Aerosol Med Pulm Drug Deliv. 2016;29(2):196–206. [PubMed: 26447531]
80. Delvadia RR, Longest PW, Hindle M, et al. In Vitro Tests for Aerosol Deposition. III: Effect of Inhaler insertion angle on aerosol deposition. J Aerosol Med Pulm Drug Deliv. 2013;26(3):145–156. [PubMed: 23025452]

81. Matida EA, Finlay WH, Grgic LB. Improved numerical simulation of aerosol deposition in an idealized mouth-throat. J Aerosol Sci. 2004;35:1–19.

82. Longest PW, Hindle M, Das Choudhuri S, et al. Numerical simulations of capillary aerosol generation: CFD model development and comparisons with experimental data. Aerosol Science and Technology. 2007;41(10):952–973.

83. Hindle M, Longest PW. Quantitative analysis and design of a spray aerosol inhaler. Part 2: Improvements in mouthpiece performance. J Aerosol Med Pulm Drug Deliv. 2013;26(5):237–247. [PubMed: 23098326]

84. Longest PW, Hindle M. Quantitative analysis and design of a spray aerosol inhaler. Part 1: Effects of dilution air inlets and flow paths. J Aerosol Med Pulm Drug Deliv. 2009;22(3):271–283. [PubMed: 19466904]

85. Longest PW, Hindle M, Das Choudhuri S. Effects of generation time on spray aerosol transport and deposition in models of the mouth-throat geometry. J Aerosol Med Pulm Drug Deliv. 2009;22(3): 67–84. [PubMed: 18956949]

86. Longest PW, Hindle M, Das Choudhuri S, et al. Developing a better understanding of spray system design using a combination of CFD modeling and experiment In: Dalby RN, Byron PR, Peart J, et al., editors. Proceedings of Respiratory Drug Delivery 2008. Illinois: Davis Healthcare International Publishing; 2008 p. 151–163.

87. Longest PW, Oldham MJ. Numerical and experimental deposition of fine respiratory aerosols: Development of a two-phase drift flux model with near-wall velocity corrections. Aerosol Science. 2008;39:48–70.*Provides valuable data to validate CFD deposition predictions on a mm-scale grid and a highly efficient deposition model for small particles

88. Longest PW, Vinchurkar S. Validating CFD predictions of respiratory aerosol deposition: effects of upstream transition and turbulence. J Biomech. 2007;40(2):305–316. [PubMed: 16533511] *Illustrates complexities associated with highly localized validation of deposition

89. Longest PW, Oldham MJ. Mutual enhancements of CFD modeling and experimental data: A case study of one micrometer particle deposition in a branching airway model. Inhal Toxicol. 2006;18(10):761–772. [PubMed: 16774865] *Provides valuable data to validate CFD deposition predictions on a mm-scale grid

90. Holbrook LT, Longest PW. Validating CFD predictions of highly localized aerosol deposition in airway models: In vitro data and effects of surface properties. J Aerosol Sci. 2013;59:6–21.*Provides valuable data to validate CFD deposition predictions on a mm-scale grid and illustrates complexities with predicting highly localized deposition

91. Matida EA, DeHaan WH, Finlay WH, et al. Simulation of particle deposition in an idealized mouth with different small diameter inlets. Aerosol Science and Technology. 2003;37:924–932.

92. Bass K, Longest PW. Recommendations for simulating microparticle deposition at conditions similar to the upper airways with two-equation turbulence models. J Aerosol Sci. 2018;10.1016/j.jaerosci.2018.02.007.

93. Zhang Y, Finlay WH, Matida EA. Particle deposition measurements and numerical simulations in a highly idealized mouth-throat. J Aerosol Sci. 2004;35:789–803.

94. Tian G, Longest PW, Su G, and Hindle M Characterization of Respiratory Drug Delivery with Enhanced Condensational Growth (ECG) Using an Individual Path Model of the Entire Tracheobronchial Airways. Ann Biomed Eng. 3 2011;39(3):18. doi: 10.1007/s10439-010-0223-z.*Complete conducting airway CFD model demonstrating the benefits of controlled condensational growth aerosol delivery

95. Walenga RL, Longest PW. Current Inhalers deliver very small doses to the lower tracheobronchial airways: Assessment of healthy and constricted lungs. J Pharm Sci. 2016;105:147–159. [PubMed: 26852850] *Used CFD to demonstrate very low deposition of conventional aerosols in the small airways

96. Walenga RL, Tian G, Longest PW. Development of characteristic upper tracheobronchial airway models for testing pharmaceutical aerosol delivery. ASME Journal of Biomechanical Engineering. 2013;135(9):091010.

97. Longest PW, Tian G, Khajeh-Hosseini-Dalasm N, et al. Validating whole-airway CFD predictions of DPI aerosol deposition at multiple flow rates. J Aerosol Med Pulm Drug Deliv. 2016;29(6):461–

481. [PubMed: 27082824] *Validation of complete-airway CFD predictions with in vivo data for pharmaceutical aerosols

98. Tian G, Hindle M, Lee S, et al. Validating CFD predictions of pharmaceutical aerosol deposition with in vivo data. Pharmaceutical Research. 2015;32:3170–3187. [PubMed: 25944585] *Validation of complete-airway CFD predictions with in vivo data for pharmaceutical aerosols
99. Newman SP, Brown J, Steed KP, et al. Lung deposition of fenoterol and flunisolide delivered using a novel device for inhaled medicines. Chest. 1998;113:957–963. [PubMed: 9554631] *Valuable source of in vivo deposition data for inhalers
100. Heistracher T, Hofmann W. Physiologically realistic models of bronchial airway bifurcations. J Aerosol Sci. 1995;26(3):497–509.
101. Yeh HC, Schum GM. Models of human lung airways and their application to inhaled particle deposition. Bull Math Biology. 1980;42:461–480.
102. Phalen RF, Oldham MJ. Tracheobronchial airway structure as revealed by casting techniques. Am Rev Respir Dis. 1983;128:S1–S4.
103. Phalen RF, Yeh HC, Schum GM, et al. Application of an idealized model to morphometry of the mammalian tracheobronchial tree. Anat Rec. 1978;190:167–176. [PubMed: 629400]
104. Sauret V, Halson PM, Brown IW, et al. Study of the three-dimensional geometry of the central conducting airways in man using computed tomographic (CT) images. J Anat. 2002;2002:123–134.
105. Koblinger L, Hofmann W. Analysis of human lung morphometric data for stochastic aerosol deposition calculations. Phys Med Biol. 1985;30:541–556. [PubMed: 4011676]
106. ICRP. Human Respiratory Tract Model for Radiological Protection. Vol. 66. New York: Elsevier Science Ltd.; 1994 (Annals of the ICRP).
107. Longest PW, Vinchurkar S. Effects of mesh style and grid convergence on particle deposition in bifurcating airway models with comparisons to experimental data. Medical Engineering and Physics. 2007;29(3):350–366. [PubMed: 16814588] *Study series illustrating the importance of proper meshing techniques
108. Vinchurkar S, Longest PW. Evaluation of hexahedral, prismatic and hybrid mesh styles for simulating respiratory aerosol dynamics. Computers and Fluids. 2008;37(3):317–331.*Study series illustrating the importance of proper meshing techniques
109. Tawhai MH, Hunter P, Tschirren J, et al. CT-based geometry analysis and finite element models of the human and ovine bronchial tree. J Appl Physiol. 2004 12;97(6):2310–2321. doi: 10.1152/japplphysiol.00520.2004.; English. [PubMed: 15322064] **Valuable description of automated airway model generation routines based on medical images
110. Kleinstreuer C, Zhang Z. An Adjustable Triple-Bifurcation Unit Model for Air-Particle Flow Simulations in Human Tracheobronchial Airways [Article]. J Biomech Eng-Trans ASME. 2009 2;131(2):10. doi: 10.1115/1.3005339.; English.
111. Kolanjiyil AV, Kleinstreuer C. Nanoparticle Mass Transfer From Lung Airways to Systemic Regions-Part II: Multi-Compartmental Modeling [Article]. J Biomech Eng-Trans ASME. 2013 12;135(12):12. doi: 10.1115/1.4025333.; English.
112. Kolanjiyil AV, Kleinstreuer C. Nanoparticle Mass Transfer From Lung Airways to Systemic Regions-Part I: Whole-Lung Aerosol Dynamics [Article]. J Biomech Eng-Trans ASME. 2013 12;135(12):11. doi: 10.1115/1.4025332.; English.
113. Kolanjiyil AV, Kleinstreuer C. Computationally efficient analysis of particle transport and deposition in a human whole-lung-airway model. Part I: Theory and model validation [Article]. Comput Biol Med. 2016 12;79:193–204. doi: 10.1016/j.compbiomed.2016.10.020.; English. [PubMed: 27810625] *Development of a whole-lung-airway CFD model
114. Kolanjiyil AV, Kleinstreuer C. Computational analysis of aerosol-dynamics in a human whole-lung airway model [Article]. J Aerosol Sci. 2017 12;114:301–316. doi: 10.1016/j.jaerosci.2017.10.001.; English.
115. Kolanjiyil AV, Kleinstreuer C, Sadikot RT. Computationally efficient analysis of particle transport and deposition in a human whole-lung-airway model. Part II: Dry powder inhaler application [Article]. Comput Biol Med. 2017 5;84:247–253. doi: 10.1016/j.compbiomed.2016.10.025.; English. [PubMed: 27836120] *Application of a whole-lung-airway CFD model

116. Islam MS, Saha SC, Sauret E, et al. Pulmonary aerosol transport and deposition analysis in upper 17 generations of the human respiratory tract [Article]. J Aerosol Sci. 2017 6;108:29–43. doi: 10.1016/j.jaerosci.2017.03.004.; English.

117. Wu D, Miyawaki S, Tawhai MH, et al. A Numerical Study of Water Loss Rate Distributions in MDCT-Based Human Airway Models [Article]. Ann Biomed Eng. 2015 11;43(11):2708–2721. doi: 10.1007/s10439-015-1318-3.; English. [PubMed: 25869455]

118. Wu D, Tawhai MH, Hoffman EA, et al. A Numerical Study of Heat and Water Vapor Transfer in MDCT-Based Human Airway Models [Article]. Ann Biomed Eng. 2014 10;42(10):2117–2131. doi: 10.1007/s10439-014-1074-9.; English. [PubMed: 25081386]

119. Yin YB, Choi JW, Hoffman EA, et al. A multiscale MDCT image-based breathing lung model with time-varying regional ventilation [Article]. J Comput Phys. 2013 7;244:168–192. doi: 10.1016/j.jcp.2012.12.007.; English. [PubMed: 23794749]

120. Tawhai MH, Pullan AJ, Hunter PJ. Generation of an anatomically based three-dimensional model of the conducting airways. Ann Biomed Eng. 2000 Jul;28(7):793–802. doi: Doi 10.1114/1.1289457.; English. [PubMed: 11016416]

121. Tgavalekos NT, Tawhai M, Harris RS, et al. Identifying airways responsible for heterogeneous ventilation and mechanical dysfunction in asthma: an image functional modeling approach. Journal Of Applied Physiology. 2005 12;99(6):2388–2397. [PubMed: 16081622] **Excellent study that synthesizes imaging and complete-airway ventilation models to make valuable predictions about asthmatic lungs

122. Vinchurkar S, De Backer L, Vos W, et al. A case series on lung deposition analysis of inhaled medication using functional imaging based computational fluid dynamics in asthmatic patients: effect of upper airway morphology and comparison with in vivo data [Article]. Inhal Toxicol. 2012 1;24(2):81–88. doi: 10.3109/08958378.2011.644351.; English. [PubMed: 22260527]

123. Usmani OS, Barnes PJ. Assessing and treating small airways disease in asthma and chronic obstructive pulmonary disease. Annals of Medicine. 2012 3;44(2):146–156. [PubMed: 21679101]

124. Van den Berge M, Ten Hacken NHT, Van der Wiel E, et al. Treatment of the bronchial tree from beginning to end: targeting small airway inflammation in asthma. Allergy. 2013;68(1):16–26. [PubMed: 23210509]

125. Kenjereš S, Tjin JL. Numerical simulations of targeted delivery of magnetic drug aerosols in the human upper and central respiratory system: a validation study. Royal Society open science. 2017;4(12):170873. [PubMed: 29308230]

126. Xie Y, Zeng P, Siegel R, et al. Magnetic deposition of aerosols composed of aggregated superparamagnetic nanoparticles. Pharmaceutical Research. 2010;27(5):855–865. [PubMed: 20198407]

127. Xie YY, Longest PW, Xu YH, et al. In vitro and in vivo lung deposition of coated magnetic aerosol particles. Journal of Pharmaceutical Sciences. 2010 11;99(11):4658–4668. [PubMed: 20845463]

128. Hindle M, Longest PW. Evaluation of enhanced condensational growth (ECG) for controlled respiratory drug delivery in a mouth-throat and upper tracheobronchial model. Pharmaceutical Research. 2010;27(9):1800–1811. [PubMed: 20454837]

129. Longest PW, Hindle M. CFD simulations of enhanced condensational growth (ECG) applied to respiratory drug delivery with comparisons to in vitro data. J Aerosol Sci. 2010;41:805–820. doi: doi:10.1016/j.jaerosci.2010.04.006. [PubMed: 20835406]

130. Hindle M, Longest PW. Condensational growth of combination drug-excipient submicrometer particles for targeted high efficiency pulmonary delivery: Evaluation of formulation and delivery device. Journal of Pharmacy and Pharmacology. 2012;64(9):1254–1263. doi: DOI: 10.1111/j.2042-7158.2012.01476.x. [PubMed: 22881438]

131. Longest PW, Hindle M. Numerical model to characterize the size increase of combination drug and hygroscopic excipient nanoparticle aerosols. Aerosol Science and Technology. 2011;45:884–899. [PubMed: 21804683]

132. Longest PW, Tian G, Li X, et al. Performance of combination drug and hygroscopic excipient submicrometer particles from a softmist inhaler in a characteristic model of the airways. Ann Biomed Eng. 2012;40(12):2596–2610. [PubMed: 22820981]
133. Tian G, Longest PW, Li X, et al. Targeting aerosol deposition to and within the lung airways using excipient enhanced growth. J Aerosol Med Pulm Drug Deliv. 2013;26(5):248–265. [PubMed: 23286828] *Implemented CFD to demonstrate targeted lung deposition with controlled condensational growth
134. Longest PW, Golshahi L, Hindle M. Improving pharmaceutical aerosol delivery during noninvasive ventilation: Effects of streamlined components. Ann Biomed Eng. 2013;41(6):1217–1232. [PubMed: 23423706]
135. Longest PW, Tian G, Hindle M. Improving the lung delivery of nasally administered aerosols during noninvasive ventilation - An application of enhanced condensational growth (ECG). J Aerosol Med Pulm Drug Deliv. 2011;24(2):103–118, DOI: 10.1089/jamp.2010.0849. [PubMed: 21410327]
136. Walenga RL, Tian G, Hindle M, et al. Variability in nose-to-lung aerosol delivery. J Aerosol Sci. 2014;78:11–29. [PubMed: 25308992] *Application of CFD to address intersubject variability in airway deposition
137. Golshahi L, Tian G, Azimi M, et al. The use of condensational growth methods for efficient drug delivery to the lungs during noninvasive ventilation high flow therapy. Pharmaceutical Research. 2013;30:2917–2930. [PubMed: 23801087]
138. Golshahi L, Walenga RL, Longest PW, et al. Development of a transient flow aersol mixer-heater system for lung delivery of nasally administered aerosols using a nasal cannula. Aerosol Science and Technology. 2014;48:1009–1021.
139. Longest PW, Walenga RL, Son Y-J, et al. High efficiency generation and delivery of aerosols through nasal cannula during noninvasive ventilation. J Aerosol Med Pulm Drug Deliv. 2013;26(5):266–279. [PubMed: 23273243]
140. Golshahi L, Longest PW, Azimi M, et al. Intermittent aerosol delivery to the lungs during high flow nasal cannula therapy. Respiratory Care. 2014;59(10):1476–1486. [PubMed: 24917454]
141. Longest PW, Golshahi L, Behara SRB, et al. Efficient nose-to-lung (N2L) aerosol delivery with a dry powder inhaler. J Aerosol Med Pulm Drug Deliv. 2015;28(3):189–201. [PubMed: 25192072]
142. Walenga RL, Longest PW, Kaviratna A, et al. Aerosol drug delivery during noninvasive positive pressure ventilation: Effects of intersubject variability and excipient enhanced growth. J Aerosol Med Pulm Drug Deliv. 2017;30(3):190–205. [PubMed: 28075194]
143. Rubin BK, Fink JB. Aerosol therapy for children. Respir Care Clin N Am. 2001;7(2):175–213. [PubMed: 11517020]
144. Fink JB. Aerosol delivery to ventilated infant and pediatric patients. Respiratory Care. 2004;49(6):653–665. [PubMed: 15165300]
145. Fok TF, Monkman S, Dolovich M, et al. Efficiency of aerosol medication delivery from a metered dose inhaler versus jet nebulizer in infants with bronchopulmonary dysplasia. Pediatric Pulmonology. 1996 5;21(5):301–309. [PubMed: 8726155]
146. Goralski JL, Davis SD. Breathing easier: Addressing the challenges of aerosolizing medications to infants and preschoolers. Respiratory Medicine. 2014;108(8):1069–1074. [PubMed: 25012949]
147. Everard ML. Inhaler devices in infants and children: Challenges and solutions. Journal of Aerosol Medicine-Deposition Clearance and Effects in the Lung. 2004 Sum;17(2):186–195.
148. DiBlasi RM. Clinical controversies in aerosol therapy for infants and children. Respiratory Care. 2015;60(6):894–916. [PubMed: 26070582]
149. Ari A, Atalay OT, Harwood R, et al. Influence of Nebulizer Type, Position, and Bias Flow on Aerosol Drug Delivery in Simulated Pediatric and Adult Lung Models During Mechanical Ventilation. Respiratory Care. 2010 7;55(7):845–851. [PubMed: 20587095]
150. El Taoum KK, Xi J, Kim JW, et al. In vitro evaluation of aerosols delivered via the nasal route. Respiratory care. 2015:respcare. 03606.

151. Carrigy NB, Ruzycki CA, Golshahi L, et al. Pediatric in vitro and in silico models of deposition via oral and nasal inhalation. J Aerosol Med Pulm Drug Deliv. 2014;27(3):149–169. [PubMed: 24870701]

152. Xi J, Berlinski A, Zhou Y, et al. Breathing resistance and ultrafine particle deposition in nasalâ-laryngeal airways of a newborn, an infant, a child, and an adult. Ann Biomed Eng. 2012;40(12): 2579–2595. [PubMed: 22660850]

153. Xi J, Si X, Zhou Y, et al. Growth of nasal and laryngeal airways in children: implications in breathing and inhaled aerosol dynamics. Respiratory Care. 2014;59(2):263–273. [PubMed: 23821760]

154. Xi JX, Si XH, Kim JW, et al. Simulation of airflow and aerosol deposition in the nasal cavity of a 5-year-old child. J Aerosol Sci. 2011 3;42(3):156–173.

155. Xi J, Longest PW. Characterization of submicrometer aerosol deposition in extrathoracic airways during nasal exhalation. Aerosol Science and Technology. 2009;43:808–827.

156. Shakked T, Broday DM, Katoshevski D, et al. Administration of aerosolized drugs to infants by a hood: A three-dimensional numerical study. Journal of Aerosol Medicine-Deposition Clearance and Effects in the Lung. 2006 Win;19(4):533–542.

157. Longest PW, Azimi M, Hindle M. Optimal delivery of aerosols to infants during mechanical ventilation. J Aerosol Med Pulm Drug Deliv. 2014;27(5):371–385. [PubMed: 24299500]

158. Longest PW, Tian G. Development of a new technique for the efficient delivery of aerosolized medications to infants on mechanical ventilation. Pharmaceutical Research. 2015;32:321–336. [PubMed: 25103332]

159. Chen WH, Lee KH, Mutuku JK, et al. Flow Dynamics and PM2.5 Deposition in Healthy and Asthmatic Airways at Different Inhalation Statuses [Article]. Aerosol Air Qual Res. 2018 4;18(4):866–883. doi: 10.4209/aaqr.2018.02.0058. English.

160. De Backer JW, Vos WG, Devolder A, et al. Computational fluid dynamics can detect changes in airway resistance in asthmatics after acute bronchodilation [Article]. J Biomech. 2008;41(1):106–113. doi: 10.1016/j.jbiomech.2007.07.009. English. [PubMed: 17698073] **Illustrates the important contribution of functional modeling in which CFD metrics can be applied as biomarkers for disease diagnosis, progression and treatment

161. De Backer JW, Vos WG, Vinchurkar SC, et al. Validation of Computational Fluid Dynamics in CT-based Airway Models with SPECT/CT. Radiology. 2010 12;257(3):854–862. [PubMed: 21084417]

162. Vos W, De Backer J, Poli G, et al. Novel Functional Imaging of Changes in Small Airways of Patients Treated with Extrafine Beclomethasone/Formoterol [Article]. Respiration. 2013;86(5): 393–401. doi: 10.1159/000347120. English. [PubMed: 23595105] **Illustrates the important contribution of functional modeling in which CFD metrics can be applied as biomarkers for disease diagnosis, progression and treatment

163. Greenblatt EE, Winkler T, Harris RS, et al. Regional Ventilation and Aerosol Deposition with Helium-Oxygen in Bronchoconstricted Asthmatic Lungs [Article]. J Aerosol Med Pulm Drug Deliv. 2016 6;29(3):260–272. doi: 10.1089/jamp.2014.1204. English. [PubMed: 26824777]

164. Lalas A, Nousias S, Kikidis D, et al. Substance deposition assessment in obstructed pulmonary system through numerical characterization of airflow and inhaled particles attributes [Article; Proceedings Paper]. BMC Med Inform Decis Mak. 2017 12;17:20. doi: 10.1186/s12911-017-0561-y. English. [PubMed: 28219437]

165. Martonen TB, Guan XF. Effects of tumors on inhaled pharmacologic drugs I. Flow patterns. Cell Biochemistry And Biophysics. 2001;35(3):233–243. [PubMed: 11894843]

166. Srivastav VK, Kumar A, Shukla SK, et al. Airflow and Aerosol-Drug Delivery in a CT Scan Based Human Respiratory Tract with Tumor Using CFD [Article]. J Appl Fluid Mech. 2014 4;7(2):345–356. English.

167. Xi JX, Kim J, Si XHA, et al. CFD Modeling and Image Analysis of Exhaled Aerosols due to a Growing Bronchial Tumor: towards Non-Invasive Diagnosis and Treatment of Respiratory Obstructive Diseases [Article]. Theranostics. 2015;5(5):443–455. doi: 10.7150/thno.11107. English. [PubMed: 25767612]

168. Xi JX, Si XHA, Kim J, et al. Exhaled Aerosol Pattern Discloses Lung Structural Abnormality: A Sensitivity Study Using Computational Modeling and Fractal Analysis [Article]. PLoS One. 2014 8;9(8):12. doi: 10.1371/journal.pone.0104682. English.

169. De Backer J, Vos W, Vinchurkar S, et al. The Effects of Extrafine Beclometasone/Formoterol (BDP/F) on Lung Function, Dyspnea, Hyperinflation, and Airway Geometry in COPD Patients: Novel Insight Using Functional Respiratory Imaging [Article]. J Aerosol Med Pulm Drug Deliv. 2015 4;28(2):88–99. doi: 10.1089/jamp.2013.1064. English. [PubMed: 25004168]

170. De Backer LA, Vos W, De Backer J, et al. The acute effect of budesonide/formoterol in COPD: a multi-slice computed tomography and lung function study [Article]. European Respiratory Journal. 2012 8;40(2):298–305. doi: 10.1183/09031936.00072511. English. [PubMed: 22183484]

171. De Backer LA, Vos WG, Salgado R, et al. Functional imaging using computer methods to compare the effect of salbutamol and ipratropium bromide in patient-specific airway models of COPD [Article]. Int J Chronic Obstr Pulm Dis. 2011;6:637–646. doi: 10.2147/copd.s21917. English.

172. Oakes JM, Marsden AL, Grandmont C, et al. Airflow and particle deposition simulations in health and emphysema: From in vivo to in silico animal experiments. Ann Biomed Eng. 2014 4;42(4):899–914. doi: 10.1007/s10439-013-0954-8. [PubMed: 24318192] **Excellent modeling study including the effect of diseased airways, importance of realistic ventilation boundary conditions and comparisons to *in vivo* data

173. Sul B, Oppito Z, Jayasekera S, et al. Assessing Airflow Sensitivity to Healthy and Diseased Lung Conditions in a Computational Fluid Dynamics Model Validated In Vitro. J Biomech Eng-T Asme. 2018 5;140(5). English.

174. Awadalla M, Miyawaki S, Abou Alaiwa MH, et al. Early Airway Structural Changes in Cystic Fibrosis Pigs as a Determinant of Particle Distribution and Deposition [Article]. Ann Biomed Eng. 2014 4;42(4):915–927. doi: 10.1007/s10439-013-0955-7. English. [PubMed: 24310865]

175. Bos AC, Van Holsbeke C, De Backer JW, et al. Patient-specific modeling of regional antibiotic concentration levels in airways of patients with cystic fibrosis: Are we dosing high enough? PLoS One. 2015;10(3):e0118454. [PubMed: 25734630] **Excellent study using CFD to determine the local dose of inhaled antibiotics

176. Bäckman P, Arora S, Couet W, et al. Advances in experimental and mechanistic computational models to understand pulmonary exposure to inhaled drugs. European Journal of Pharmaceutical Sciences. 2018;113:41–52. [PubMed: 29079338]

177. Rygg A, Hindle M, Longest PW. Linking suspension nasal spray drug deposition patterns to pharmacokinetic profiles: A proof-of-concept study using computational fluid dynamics. Journal of Pharmaceutical Sciences. 2016;105:1995–2004. [PubMed: 27238495] *Illustrates validation of CFD absorption predictions with in vivo PK data for nasal sprays

178. Bush ML, Frederick CB, Kimbell JS, et al. A CFD–PBPK hybrid model for simulating gas and vapor uptake in the rat nose. Toxicology and applied pharmacology. 1998;150(1):133–145. [PubMed: 9630462]

179. Rygg A, Hindle M, Longest PW. Absorption and clearance of pharmaceutical aerosols in the human nose: Effects of nasal spray suspension particle size and properties. Pharmaceutical Research. 2016;33:909–921. [PubMed: 26689412] *Development and application of a deposition, absorption and clearance CFD model for nasal sprays

180. Rygg A, Longest PW. Absorption and clearance of pharmaceutical aerosols in the human nose: Development of a CFD model. J Aerosol Med Pulm Drug Deliv. 2016;29(5):416–431. [PubMed: 26824178] *Development and application of a deposition, absorption and clearance CFD model for nasal sprays

181. Longest PW, Rygg A, Hindle M. Bioequivalence testing: Can systemic pharmacokinetic profiles from corticosteriod nasal sprays be used to elucidate local drug deposition within the nose? Respiratory Drug Delivery 2016. 2016;1:175–184.

182. Gelb AF, Taylor CF, Nussbaum E, et al. Alveolar and airway sites of nitric oxide inflammation in treated asthma. American Journal of Respiratory and Critical Care Medicine. 2004;170(7):737–741. [PubMed: 15229098]

183. Usmani OS. Treating the small airways. Respiration. 2012;84(6):441–453. [PubMed: 23154684]

184. Delvadia R, Longest PW, Byron PR. In vitro tests for aerosol deposition. I. Scaling a physical model of the upper airways to predict drug deposition variation in normal humans. Journal of Aerosol Medicine. 2012;25(1):32–40.

185. Behara SRB, Longest PW, Farkas DR, et al. Development and comparison of new high-efficiency dry powder inhalers for carrier-free formulations. Journal of Pharmaceutical Sciences. 2014;103:465–477. [PubMed: 24307605]

186. Longest PW, Son Y-J, Holbrook LT, et al. Aerodynamic factors responsible for the deaggregation of carrier-free drug powders to form micrometer and submicrometer aerosols. Pharmaceutical Research. 2013;30:1608–1627. doi: DOI: 10.1007/s11095-013-1001-z. [PubMed: 23471640]

187. Son Y-J, Longest PW, Tian G, et al. Evaluation and modification of commercial dry powder inhalers for the aerosolization of submicrometer excipient enhanced growth (EEG) formulation. European Journal of Pharmaceutical Sciences. 2013;49:390–399. [PubMed: 23608613]

188. Olsson B, Berg E, Svensson M. Comparing aerosol size distributions that penetrate mouth-throat models under realistic inhalation conditions. Respiratory Drug Delivery 2010 2010:225–234.

189. Longest PW, Hindle M. Condensational growth of combination drug-excipient submicrometer particles: Comparison of CFD predictions with experimental results. Pharmaceutical Research. 2012;29(3):707–721. [PubMed: 21948458]

190. Son Y-J, Longest PW, Hindle M. Aerosolization characteristics of dry powder inhaler formulations for the excipient enhanced growth (EEG) application: Effect of spray drying process conditions on aerosol performance. International Journal of Pharmaceutics. 2013;443:137–145. [PubMed: 23313343]

191. Tian G, Hindle M, Longest PW. Targeted lung delivery of nasally administered aerosols. Aerosol Science and Technology. 2014;48(4):434–449. [PubMed: 24932058]

192. Longest PW. CFD and hybrid deposition modeling: When and why the approach is useful. Respiratory Drug Delivery 2018. 2018;1:123–136.

193. Behara SRB, Farkas DR, Hindle M, et al. Development of a high efficiency dry powder inhaler: effects of capsule chamber design and inhaler surface modifications. Pharmaceutical Research. 2014;31:360–372. [PubMed: 23949304]

194. Newman S, Salmon A, Nave R, et al. High lung depostion of 99mTc-labeled ciclesonide administered via HFA-MDI to patients with asthma. Respiratory Medicine. 2006;100:375–384. [PubMed: 16275052] *Valuable source of in vivo deposition data for inhalers

195. Katz I, Pichelin M, Montesantos S, et al. The influence of lung volume during imaging on CFD within realistic airway models. Aerosol Science and Technology. 2017;51(2):214–223.

196. Scheinherr A, Bailly L, Boiron O, et al. Realistic glottal motion and airflow rate during human breathing. Med Eng Phys. 2015;37(9):829–839. [PubMed: 26159687]

197. Lee SL, Adams WP, Li BV, et al. In Vitro Considerations to Support Bioequivalence of Locally Acting Drugs in Dry Powder Inhalers for Lung Diseases. AAPS Journal. 2009 3;11(3):414–423. [PubMed: 19495991]

198. Borgstrom L, Olsson B, Thorsson L. Degree of throat deposition can explain the variability in lung deposition of inhaled drugs. Journal of Aerosol Medicine. 2006;19:473–483. [PubMed: 17196076]

199. Heyder J, Gebhart J, Rudolf G, et al. Deposition of particles in the human respiratory tract in the size range of 0.005 – 15 microns. J Aerosol Sci. 1986;17(5):811–825.

200. Stahlhofen W, Rudolf G, James A. Intercomparison of experimental regional aerosol deposition data. Journal of Aerosol Medicine. 1989;2(3):285–308.

201. Grgic B, Finlay WH, Burnell PKP, et al. In vitro intersubject and intrasubject deposition measurements in realistic mouth-throat geometries. J Aerosol Sci. 2004 8;35(8):1025–1040.

202. Golshahi L, Finlay WH, Olfert JS, et al. Deposition of inhaled ultrafine aerosols in replicas of nasal airways of infants. Aerosol Science and Technology. 2010;44:741–752.

203. Storey-Bishoff J, Noga M, Finlay WH. Deposition of micrometer-sized aerosol particles in infant nasal airway replicas. Aerosol Science. 2008;39:1055–1065.

204. Tavernini S, Church TK, Lewis DA, et al. Deposition of micrometer-sized aerosol particles in neonatal nasal airway replicas. Aerosol Science and Technology. 2018;52(4):407–419.

205. Tgavalekos NT, Musch G, Harris RS, et al. Relationship between airway narrowing, patchy ventilation and lung mechanics in asthmatics. European Respiratory Journal. 2007;29(6):1174–1181. [PubMed: 17360726]

206. Pozin N, Montesantos S, Katz I, et al. A tree-parenchyma coupled model for lung ventilation simulation. International Journal for Numerical Methods in Biomedical Engineering. 2017;33(11):e2873.

207. Corcoran TE. Imaging in aerosol medicine. Respiratory Care. 2015;60(6):850–857. [PubMed: 26070579]

Article highlights

- Computational fluid dynamics (CFD) is a scientific simulation technique that is capable of providing spatially and temporally resolved predictions of many aspects related to respiratory drug delivery.
- A key to successful use of CFD is conducting an analysis concurrent with *in vitro* experiments.
- Regional deposition models have provided an improved understanding of pharmaceutical aerosol delivery for several decades.
- Complete-airway deposition modeling is now being used in some cases to better understand existing respiratory drug delivery techniques and to develop new targeted delivery strategies.
- New strategies in development using concurrent analysis include controlled condensational growth and nose-to-lung aerosol administration for infants and children.
- We envision future applications of CFD deposition modeling to reduce the need for human subject testing in developing new devices and formulations, to help establish bioequivalence for the accelerated approval of generic inhalers, and to provide valuable new insights related to drug dissolution and clearance leading to microdosimetry maps of drug absorption throughout the lungs.

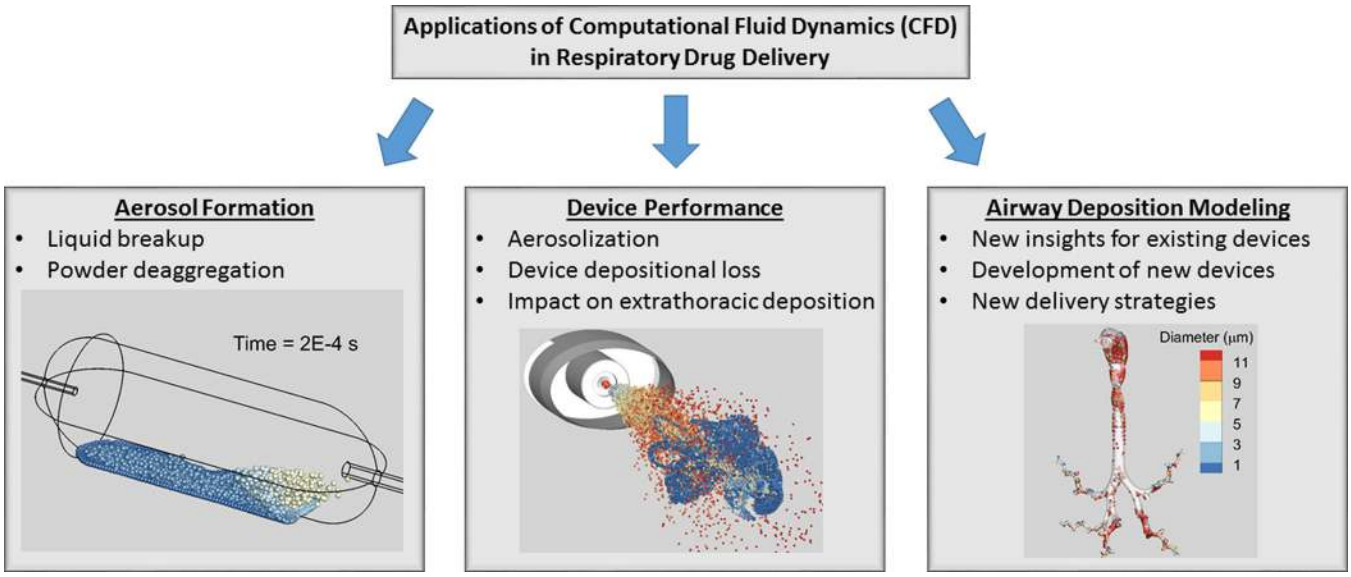

Figure 1.

Primary areas in which computational fluid dynamics (CFD) has been applied to respiratory drug delivery including the simulation of (*i*) liquid and powder aerosol formation, (*ii*) device design and performance, and (*iii*) airway deposition modeling.

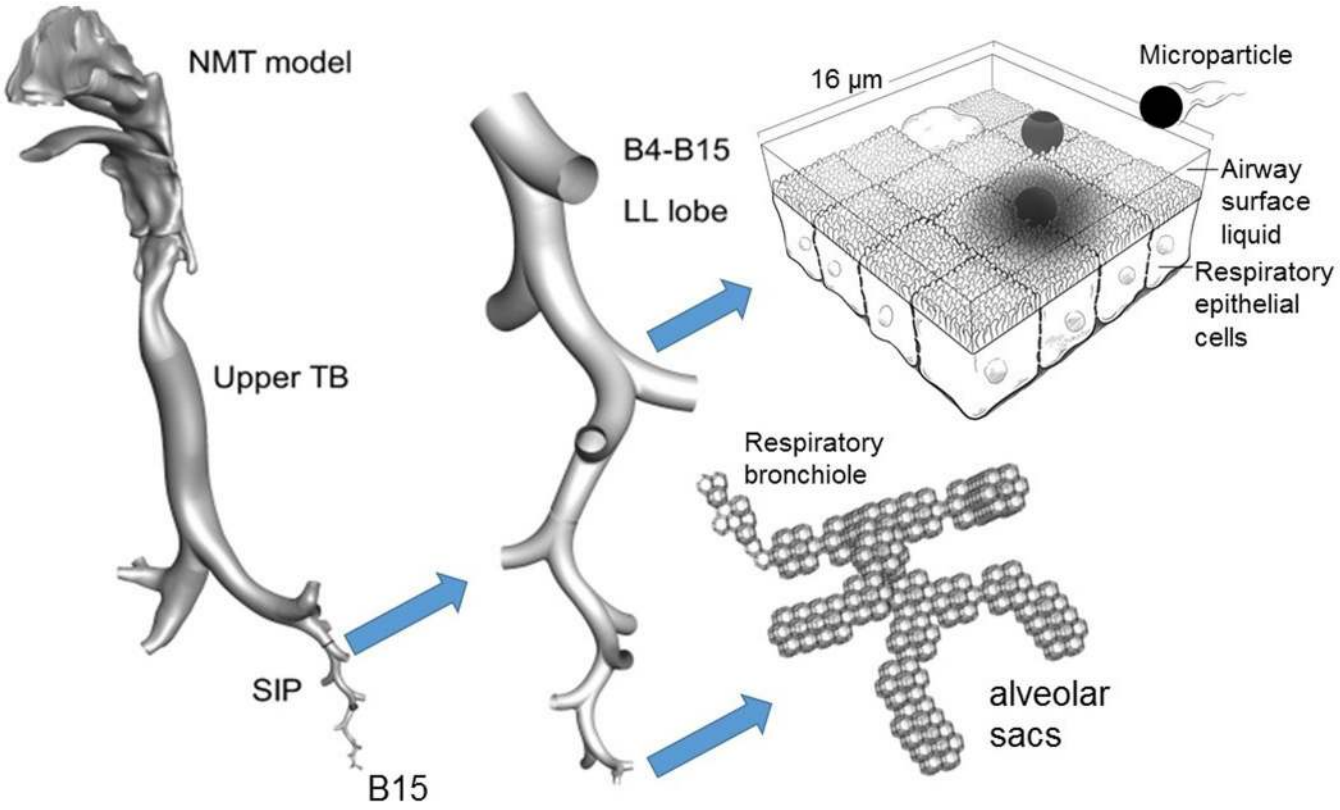

Figure 2.

Overview of complete-airway CFD simulations beginning with the site of aerosol formation and continuing through particle deposition. Using the stochastic individual pathway (SIP) approach [13, 28, 55], an ensemble of airway paths is selected within each lung lobe. Only one SIP unit is illustrated in the left lower lobe in this figure. The model of the alveolar region is composed of a representative acinar segment beginning with a respiratory bronchiole and continuing through the alveolar sacs [56]. Complete-airway simulations can be continued through post-deposition transport [14].

Portions redrawn and adapted from Longest and Hindle [14] with permission of Springer Nature.

B#: bifurcation number; LL: left lower; NMT: nose-mouth-throat airway

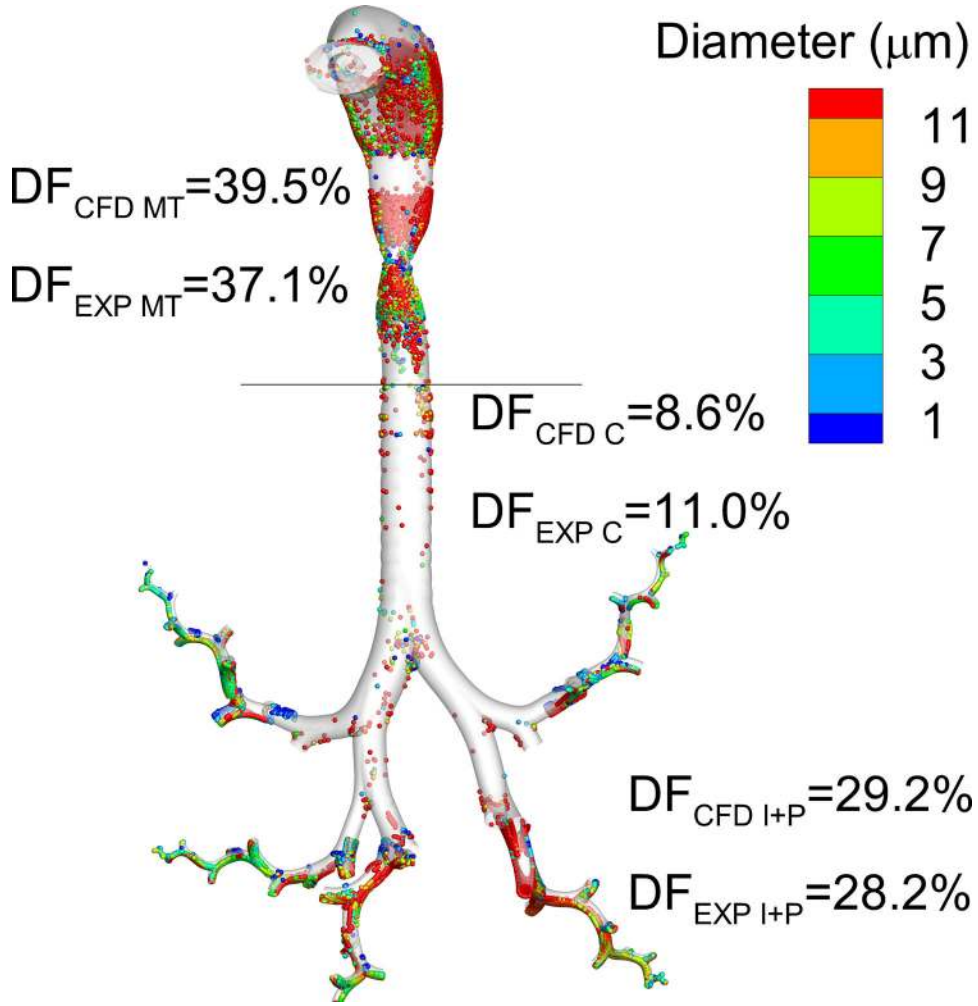

Figure 3.

Comparison of *in vivo* [99] and CFD [98] predictions of deposition fraction (DF) in different regions of the airways for the Respimat inhaler with a fenoterol formulation. Reasonable agreement is achieved at the level of available *in vivo* data resolution including the mouth-throat (MT), central (C), and intermediate + peripheral (I+P) airways with one SIP unit considered in each lung lobe. Diseased airways or more refined deposition predictions will require additional SIP pathways.

Reproduced from Tian et al. [98] with permission of Springer Nature.

EXP: in vivo experimental results; CFD: computational fluid dynamics predictions

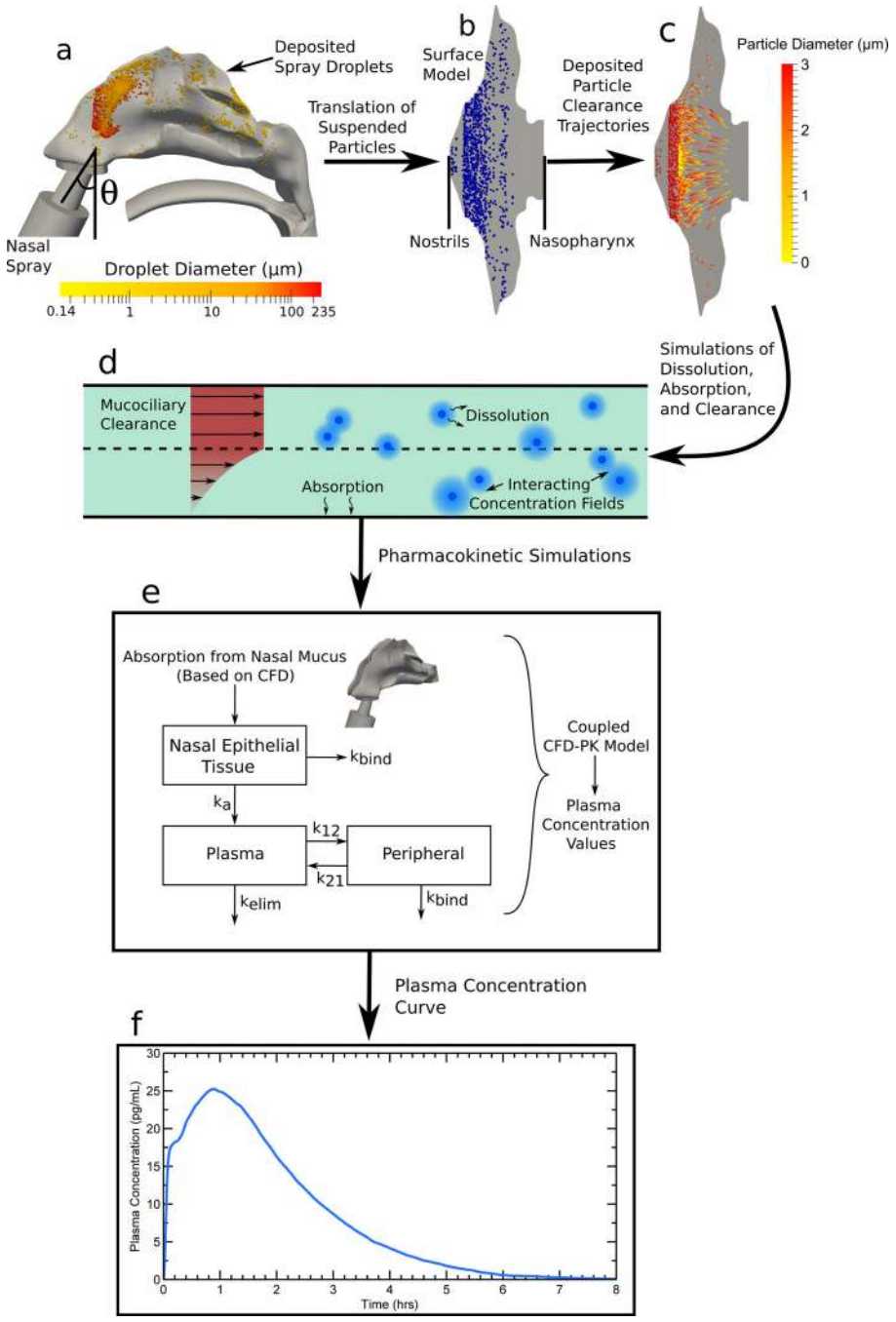

Figure 4.

Overall methodology for CFD-PK simulations of a nasal spray application from Rygg et al. [177] and Longest et al. [181]. Particle deposition data in the (a) 3D model of the nose was mapped onto the (b) interior surface model. CFD simulations accounted for (c) particle movement due to mucociliary clearance, and (d) particle dissolution, diffusion and drug absorption at the epithelial surface. Pharmacokinetic simulations (e) provided plasma concentration vs time profiles (f).

Reproduced with permission from Respiratory Drug Delivery 2016 [181], Virginia Commonwealth University and RDD Online.

PK: pharmacokinetics

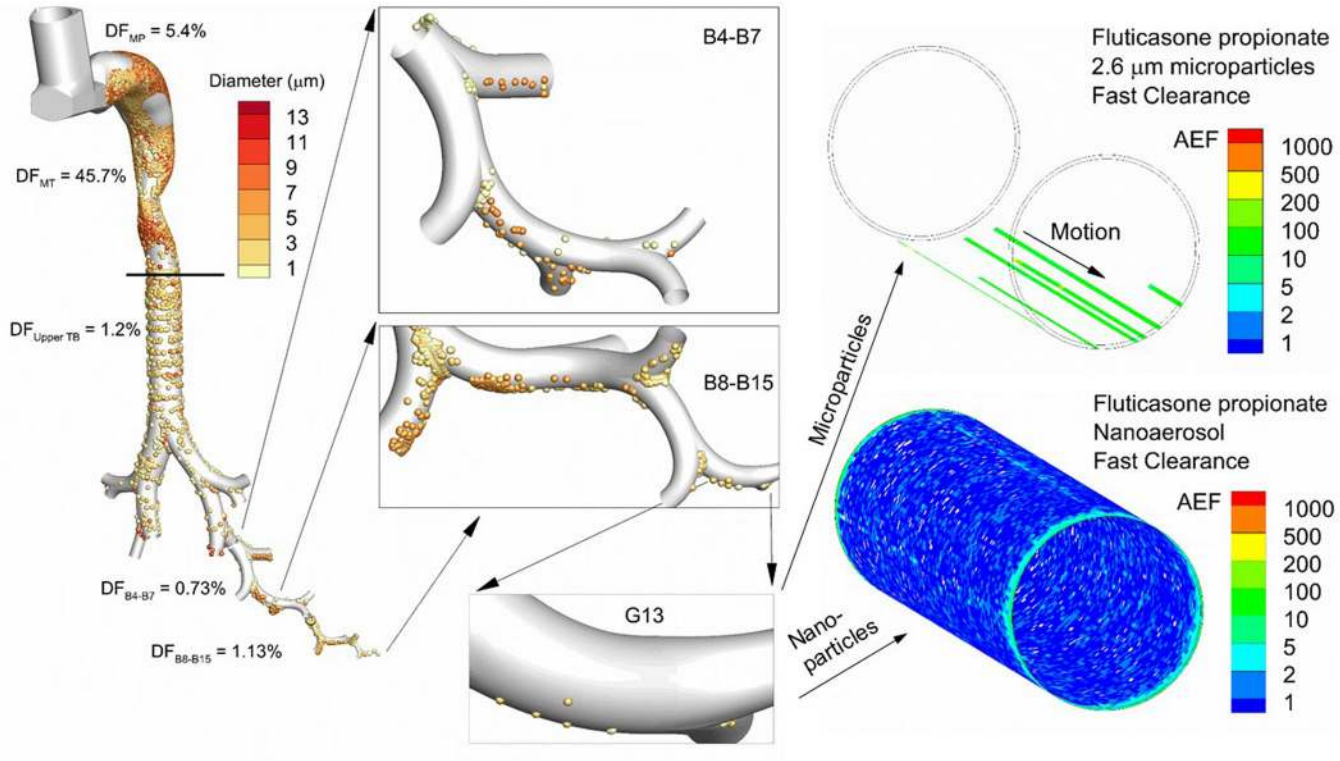

Figure 5.

Overview of complete-airway modeling beginning with the inhaler and progressing through simulation of corticosteroid dissolution, absorption and clearance in airway generation G13. Deposition fraction (DF) from Walenga et al. [95] for the Flovent HFA MDI in the device mouthpiece (MP) and different regions of the conducting airways including the mouth-throat (MT), upper tracheobronchial (TB) region containing the main bifurcation (B1) through B3, and bifurcation segments B4–B7 and B8–B15. Magnified views of deposited particles in the lower airways are shown in the panels, including the deposition of particles in the size range of 1–3 μm in airway generation G13. Panels on the right side illustrate post-deposition absorption and clearance of the predicted deposited drug mass in G13 formulated as either a microparticle or true nanoaerosol. Values of the absorption enhancement factor (AEF) into respiratory epithelial cells are contoured, with AEF values below 0.1 excluded (i.e., left clear). AEF represents the local absorption in a 16×16 matrix of surface epithelial cells normalized by the total area-averaged absorption in the small airway geometry. An AEF of 1000 in a single element indicates 1000 times more inhaled corticosteroid absorption in a 16×16 matrix of cells compared to the total dose per total area.

Adapted from Longest and Hindle [14] with permission of Springer Nature.